



Illinois State Water Survey

Main Office • 2204 Griffith Drive • Champaign, IL 61820-7495 • Tel (217) 333-2210 • Fax (217) 333-6540
Peoria Office • P.O. Box 697 • Peoria, IL 61652-0697 • Tel (309) 671-3196 • Fax (309) 671-3106



Hydrology Division • Tel (217) 333-4300 • Fax (217) 244-0777

September 11, 1997

Mark Leibrock
Waste Management Inc.
2 Westbrook Corporate Center, Suite 1000
Westchester, IL 60154

US EPA RECORDS CENTER REGION 5



408601

Dear Mr. Leibrock:

Enclosed is a copy of Gus Vythoulkas's thesis on the composition of slag and its significance to ground water. Gus performed this work while working for the Illinois State Water Survey and attending the University of Illinois-Chicago. We are currently converting this report, as well as analyses from our other activities, into journal articles and a web page. I have also included three analyses showing the chemical changes as ground water from a slag pile is discharged into a wetland.

The thesis details the mineralogical and metal composition of slag and how it might weather and react in a ground water system. The unweathered cores of the steel slag samples contain lime, calcium-silicate minerals, and steel droplets. As this material is exposed to air and water, it reacts to form a weathering rind of calcite, silica, and pyrite. A large amount of hydroxyl ions are released which can drive the pH up over 12. Iron and other metals are also released and can be found in the structure of the weathering products. Samples from a modern iron (blastfurnace) slag show the same general behavior except the metal content is significantly less.

The central question to wetland habitats is the fate of the high pH and metals that come out of the slag. This question is part of the focus of our current studies in the area. From our ground water analyses we see a relatively small amount of metal in the water compared to what is in the slag. The bulk of the metals are likely being sorbed or reprecipitated within the slag pile. The weathering rind on the slag will also build up with time, thus reducing the weathering rate of the core slag. We are currently trying to assess what form the metals are in, what they are bound or incorporated into, and how stable the new forms are.

Because of the heterogeneous nature of the slag, ground water tends to discharge into surface waters through springs. At these springs the high pH ground water reacts with carbon dioxide in the atmosphere. This reaction lowers the pH and causes more calcite and ferric hydroxide to precipitate out which will scavenge a lot of metals. The attached analyses are from a slag pile in the area. The ground water shows a very high pH (12.65) with a high amount of calcium and some elevated levels of heavy metals. Although iron was visible at the surface, the iron level in the ground water was very low for the region. The downstream spring sample and the surface water sample from the receiving wetland show a considerable decrease in pH, calcium, and heavy metal content. We are currently analyzing the calcite precipitated from the mouth of the spring at this site. Analysis of similar precipitate from a site in Indiana shows a fairly high metal content.

Persistent elevated pHs in wetlands and ditches are a large problem throughout the Lake Calumet region because of the large amount of slag that was dumped virtually everywhere. We are currently investigating low-cost techniques to address these problem areas. Our basic idea is to lower the pH through aeration that would introduce carbon dioxide from the atmosphere. We are also proposing a hydraulic modification to the large wetland system east of Lake Calumet, including Big Marsh, that among its many benefits would be amelioration of the problems caused by ground water discharge. Concurrent with our studies of the aeration techniques is an assessment of the toxicity of the water and how it would improve at the high pH hot spots.

In general, we recognize that removing the 21 billion cubic feet of fill (according to a new US Geological Survey estimate) from over a 60 square mile area is unrealistic. I think our research will show that there are ways to easily treat the hot spots and to drastically improve habitats throughout the region.

I will keep you apprised of our further research findings as they are published. If you have any comments, please call or email me.

Sincerely,



George S. Roadcap
Associate Hydrogeologist
Office of Ground-Water Quality
Phone: (217) 333-7951
george@sparc.sws.uiuc.edu

gsr/psh

Enclosure

Table 1. Water Samples Associated with a Slag Pile in the Lake Calumet Region.

| Type of Sample | | Ground Water | Spring | Wetland |
|--------------------------------------|-----|--------------|--------|---------|
| Major Constituents (mg/L) | | | | |
| Calcium | Ca | 1067 | 147 | 72 |
| Magnesium | Mg | nd | 23.2 | 22.4 |
| Sodium | Na | 51.1 | 70.2 | 68 |
| Potassium | K | 46.5 | 44.7 | 48 |
| Chloride | Cl | 76.2 | 95 | 96.3 |
| Sulfate | SO4 | 5.3 | 114.7 | 115.3 |
| Alkalinity | ALK | 2687 | 124 | 164 |
| Dissolved Solids | TDS | 2387 | 532 | 595 |
| Organic Carbon | TOC | 11.3 | 17.3 | 12.4 |
| pH - Lab | pH | 12.65 | 9.08 | 8.11 |
| Secondary Constituents (mg/L) | | | | |
| Ammonia | NH4 | 5.016 | 0.963 | 1.273 |
| Nitrate | NO3 | 0.73 | nd | nd |
| Phosphate | PO4 | 0.009 | 0.044 | 0.273 |
| Aluminum | Al | 0.137 | 0.154 | 0.015 |
| Boron | B | 0.09 | 0.55 | 0.54 |
| Fluoride | F | 5.1 | 1.4 | 1.3 |
| Iron | Fe | 0.037 | 0.885 | 0.809 |
| Manganese | Mn | 0.008 | 0.148 | 0.158 |
| Silicon | Si | nd | 3.14 | 2.88 |
| Strontium | Sr | 3.19 | 0.619 | 0.475 |
| Trace Metals (mg/L) | | | | |
| Antimony | Sb | nd | nd | nd |
| Arsenic | As | nd | nd | nd |
| Barium | Ba | 0.374 | 0.086 | 0.062 |
| Beryllium | Be | 0.019 | nd | 0.005 |
| Cadmium | Cd | nd | nd | nd |
| Chromium | Cr | 0.043 | 0.017 | nd |
| Cobalt | Co | 0.019 | 0.007 | nd |
| Copper | Cu | 0.023 | 0.038 | nd |
| Lead | Pb | 0.029 | nd | 0.017 |
| Lithium | Li | nd | 0.043 | 0.055 |
| Mercury | Hg | nd | nd | nd |
| Molybdenum | Mo | 0.006 | nd | nd |
| Nickel | Ni | 0.05 | 0.036 | nd |
| Selenium | Se | nd | nd | nd |
| Silver | Ag | nd | nd | nd |
| Thallium | Tl | 0.31 | 0.27 | nd |
| Tin | Sn | nd | nd | nd |
| Titanium | Ti | 0.035 | 0.012 | 0.007 |
| Vanadium | V | 0.005 | 0.043 | 0.014 |
| Zinc | Zn | 0.229 | 1.51 | 0.466 |

**SLAG MATERIALS AND THEIR SIGNIFICANCE ON GROUNDWATER
GEOCHEMISTRY IN SOUTHEAST CHICAGO**

BY

KONSTANTINOS V. VYTHOULKAS
B Sc , University of Athens, Greece, 1992

THESIS

Submitted as partial fulfillment of the requirements
for the degree of Master of Science in Geological Sciences
in the Graduate College of the
University of Illinois at Chicago, 1997

Chicago, Illinois

This thesis is dedicated to my mother. Without her loving support, it would never have been accomplished

ACKNOWLEDGMENTS

I thank my advisor, Neil Sturchio for his guidance and assistance throughout the entire project. I also thank Charlie Xu for his valuable advice and comments, Steve Guggenheim for his guidance, and Gene Harris for his help on the operation of the SEM/EDS system.

I also thank George Roadcap of the Illinois State Water Survey for all of his help during the research and for financial support of this study.

KVV

TABLE OF CONTENTS

| <u>CHAPTER</u> | <u>PAGE</u> |
|---|-------------|
| I. INTRODUCTION | 1 |
| A. Purpose and summary of this study..... | 1 |
| B. Definition and classification of steel and blastfurnace slag materials..... | 1 |
| C. Slag deposits in the Lake Calumet area..... | 3 |
| D. Groundwater chemistry in the Lake Calumet area..... | 4 |
| II. METHODS..... | 11 |
| A. Sampling of slag materials. | 11 |
| 1 Monitoring well..... | 11 |
| 2 Slag piles | 12 |
| B. Characterization of slags..... | 15 |
| 1 X-ray diffraction..... | 15 |
| 2 Optical and electron microscopy..... | 15 |
| C. Batch powder-reaction experiments | 16 |
| 1. Steel slag samples..... | 16 |
| 2 Blastfurnace slag samples..... | 17 |
| III. RESULTS..... | 19 |
| A Steel slag from Lake Calumet well #2..... | 19 |
| 1. X-ray diffraction results | 19 |
| 2 Optical and electron microscopy results..... | 22 |
| 3 Batch powder-reaction results | 30 |
| 4 Geochemical modeling results | 36 |
| B. Blastfurnace slag from Koch Materials | 39 |
| 1 X-ray diffraction results..... | 39 |
| 2 Optical and electron microscopy results | 40 |
| 3. Batch powder-reaction results..... | 41 |
| 4. Geochemical modeling results..... | 53 |
| IV. DISCUSSION..... | 56 |
| A. Comparison of steel and blastfurnace slag results..... | 56 |
| 1. X-ray diffraction..... | 56 |
| 2 Optical and electron microscopy. | 57 |
| 3. Batch powder-reactions | 57 |
| B. General nature of slag weathering..... | 58 |
| C. Potential impact on groundwater chemistry..... | 66 |
| D. Suggestions for future work. | 70 |
| CITED LITERATURE | 71 |

TABLE OF CONTENTS (continued)

| <u>CHAPTER</u> | <u>PAGE</u> |
|----------------|-------------|
| VITA..... | 74 |

LIST OF TABLES

| <u>TABLE</u> | <u>PAGE</u> |
|--|-------------|
| I. GROUNDWATER CHEMISTRY OF WELL #2 NEAR LAKE CALUMET..... | 9 |
| II. INITIAL pH OF BLASTFURNACE SLAG LEACHATES (OXIC AND ANOXIC SERIES)..... | 18 |
| III. d SPACING AND RELATIVE INTENSITIES OF STEEL SLAG SAMPLES..... | 20 |
| IV. SEM/EDS ANALYSIS OF FeS ₂ IN SAMPLE S5..... | 26 |
| V. SEM/EDS ANALYSES OF THE CORE AND WEATHERED PART OF FIELD SAMPLE S3 | 27 |
| VI. SEM/EDS ANALYSES OF THE CORE AND WEATHERED PART OF FIELD SAMPLE S4..... | 28 |
| VII. CHEMICAL ANALYSES OF FIELD SAMPLE LEACHATES. | 31 |
| VIII. METAL RELEASE PER UNIT MASS WASTE OF FIELD SAMPLE LEACHATES | 35 |
| IX. PERCENTAGE DISTRIBUTION OF COMPONENTS. | 37 |
| X. d SPACING AND RELATIVE INTENSITIES OF BLASTFURNACE SLAG SAMPLES | 40 |
| XI. SEM/EDS ANALYSIS OF BLASTFURNACE SLAG (FS1A)..... | 42 |
| XII. pH MEASUREMENTS OF FRESH BLASTFURNACE SLAG..... | 43 |
| XIII. CHEMICAL ANALYSIS OF FRESH BLASTFURNACE SLAG LEACHATE - OXIC SERIES..... | 45 |
| XIV. METAL RELEASE PER UNIT MASS WASTE UNDER OXIC CONDITIONS..... | 46 |
| XV. CHEMICAL ANALYSIS OF BLASTFURNACE SLAG LEACHATE - ANOXIC SERIES | 47 |

LIST OF TABLES (continued)

| <u>TABLE</u> | <u>PAGE</u> |
|---|-------------|
| XVI METAL RELEASE PER UNIT MASS WASTE UNDER ANOXIC CONDITIONS..... | 48 |
| XVII. COMPARISON BETWEEN OXIC AND ANOXIC SERIES..... | 50 |

LIST OF FIGURES

| <u>FIGURE</u> | | <u>PAGE</u> |
|---------------|--|-------------|
| 1 | Study area map and locations of monitoring wells | 6 |
| 2 | Well log of well #2 | 8 |
| 3. | Field samples of steel slag used in the study. A penny (19 mm diameter) is shown for scale.. | 12 |
| 4 | Blastfurnace slag samples used in the study. Ball-point pen (15 cm long) shown for scale | 14 |
| 5. | Blastfurnace slag piles at Koch Materials Inc. in Indiana..... | 14 |
| 6. | Photomicrograph of sample S1 viewed under the light microscope (transmitted light) | 23 |
| 7. | Photomicrograph of the same area under the SEM (BEI mode) | 23 |
| 8 | SEM photographs (BEI mode) showing microcrystalline “pyrite” embedded in the weathered part of steel slag S5..... | 25 |
| 9. | SEM photograph showing “pyrite” crystals in the core sample SSA where steel slag was buried | 26 |
| 10. | SEM photograph (BEI mode) of field sample S3. | 29 |
| 11 | SEM photograph (BEI mode) of field sample S4.... | 29 |
| 12. | Comparison of chemical compositions of field sample leachates and well #2 groundwater | 34 |
| 13. | Batch powder-reaction experiments. Oxidic series | 51 |
| 14. | Batch powder-reaction experiments Anoxic series. | 52 |
| 15. | CaCO ₃ (calcite) precipitates in ditches near well #2..... | 63 |
| 16 | Comparison of chemical compositions of leachate S4 and well #2 groundwater | 68 |

SUMMARY

Steel slag samples from Illinois State Water Survey (ISWS) monitoring well #2, Lake Calumet, Chicago and fresh blastfurnace slag from Koch Materials Inc , Indiana were collected for the purpose of this study. The weathering mechanisms of the slag were studied to investigate the effect of their leachates on groundwater chemistry in the Lake Calumet area and steel mill slag landfills in general

Steel slag samples were collected from the borehole of ISWS monitoring well #2 and characterized using x-ray diffraction (XRD), optical microscopy, and scanning electron microscopy (SEM) with energy dispersive x-ray analysis (EDS). A weathered coating observed in all samples, revealed the presence of “calcite”, “dolomite”, and “quartz” as the major secondary phases from slag weathering. The samples were also used in batch powder-reaction experiments with dilute acid and distilled water. The pH of the leachate was high, close to 11, as a result of the dissolution of the slag constituents

Fresh blastfurnace slag samples from Koch Materials, Indiana were characterized using the same experimental methods. The samples were also used in batch powder-reaction experiments with dilute acid solutions of varied pH. The pH of the leachate was consistently high which indicates the alkaline nature of the material. The concentrations of Ca, Mg, Si, Na, K, Cl, and SO_4^{2-} in the leachates were relatively high. Sr and Ba were observed in trace concentrations.

I. INTRODUCTION

A. Purpose and summary of this study

This study was undertaken to investigate the effect of steel mill slag weathering on groundwater chemistry in the Lake Calumet area, southeast Chicago, Illinois. Partially weathered steel slag samples from Illinois State Water Survey (ISWS) monitoring well #2, Lake Calumet, and fresh blastfurnace slag from Koch Materials, Indiana, were collected. These samples were characterized using x-ray diffraction (XRD), optical microscopy, and scanning electron microscopy (SEM) with energy dispersive x-ray analysis (EDS). The samples were used in batch powder-reaction experiments with dilute acid solutions to obtain general information on possible weathering reaction mechanisms and their effects on water chemistry. Geochemical modeling of powder-reaction solution compositions was performed to gain insights as to the specific involvement of observed primary and secondary solid phases during slag weathering.

B. Definition and classification of steel and blastfurnace slag materials

Steel and blastfurnace slags are the by-products of steel mills. In the production of iron, the blastfurnace is charged with iron ore, fluxstone (limestone and/or dolomite), and coke for fuel. Slag is the name applied to the fusible material formed by the chemical reaction of a flux with the gangue of an ore, with the ash from a fuel, or with the impurities oxidized during the refining of a metal (Lankford et al, 1985a). There are two types of steel mill slags: "blastfurnace slag", that originates from the production of pig iron from the original iron ore and "steel slag", that comes from the production of steel from pig iron.

Blastfurnace slag is a chemically uniform solid in which calcium and magnesium oxides are combined in silicates and aluminosilicates. The oxides of calcium and magnesium originate mainly from the fluxstone whereas the silica and alumina come from the original iron ore. Steel slag is composed of about 50% CaO and contains more Fe and Mn than blastfurnace slag. In steel slag, the reactions between the slag constituents (feed materials) are incomplete, resulting in a chemically non-uniform solid that may contain substantial amounts of free calcium and/or magnesium oxides (Akiminsuru, 1991a).

The composition of slag varies over a wide range depending on the nature of the ore, the composition of the limestone flux, and the kind of iron being produced. These variations affect the relative contents of the four major constituents: lime, silica, alumina, and magnesia. They also affect the amounts of the minor components, such as sulfur in the form of sulfide, and ferrous and manganese oxides (Lea, 1956a). The result of this wide variation in chemical properties affects the usefulness and the value of slags for nonmetallurgical applications.

Dicalcium silicate (Ca_2SiO_4) is a major crystalline phase in slags. Dicalcium silicate has three polymorphs, α - Ca_2SiO_4 (known naturally as bredigite), β - Ca_2SiO_4 (known as larnite when found in nature) and γ - Ca_2SiO_4 . The α' or β' polymorphs are reactive and are readily hydrated whereas the γ' form is inert (Lea, 1956b).

Minerals are naturally occurring inorganic solids with defined chemical compositions and crystal structures. Slags are man-made materials and therefore the crystalline phases in slag are not minerals. However, it is more convenient to refer to these phases by their corresponding mineral names rather than their chemical formulas. In this manuscript, the mineral names are used to identify crystalline phases in slag materials.

C. Slag deposits in the Lake Calumet area

The study area is located near Lake Calumet, 15 miles south of downtown Chicago, Illinois. It is an extensive region of landfills. Before its development, the area surrounding Lake Calumet was a region of marshes. Since 1869, different solid wastes were used as landfill to convert the marshes into usable industrial and residential properties, reducing the lake to half of its original size.

The Lake Calumet area of southeast Chicago is now a heavily industrialized area. Different waste disposal practices over the past 100 years have severely altered the local environment. The large amount of solid waste poses a serious environmental threat to groundwater quality. The major industry in the region is the steel industry which has profoundly affected the landscape and environment. The most abundant types of solid waste disposed of in the region are steel mill slags and dredgings from the deepening and channelization of the Calumet River system (Colten, 1985a). Other types of waste include fly ash, solid industrial wastes, demolition debris, garbage, bricks, wood, metal scraps, concrete, and household trash.

Fifty-one disposal sites have been identified in the Lake Calumet area. These sites include sanitary landfills, on-site settling ponds, and general refuse ponds (Colten, 1985b). Waste disposal is still a large industry in the Lake Calumet area with five large municipal landfills, a large sewage plant, and several large sludge drying beds. As many as 13 sites in the area are on the Superfund priority list, making the area around Lake Calumet one of the largest and most hazardous waste sites in the nation.

Twenty-five manufacturers in the Illinois portion of the Calumet region produced iron and steel products from 1922 to 1940 (Colten, 1985c). The steel mills of the area produced a basic

slag suited for use in Portland cement. Slag deposits are generally alkaline and stable, however the addition of foreign substances can make them hazardous (Colten, 1985d). Quenching liquids (sulfuric acid and FeSO_4) derived from pickling processes were added to the hot slag to cool it down. These liquids can leach into groundwater and carry dissolved material from the slag with them. Slags contain heavy metals in high concentrations around the industrial sites in the Calumet area (Colten, 1985e). Lee (1974a) observed that if slag is placed in relatively stagnant water, in some cases the compounds leached out may cause corrosion of adjacent concrete made with ordinary Portland cement. There are no data, however, regarding the nature of these compounds.

Slag is the most abundant and most visible by-product of the steel mills that was disposed in the Lake Calumet area. Much was piled at high temperatures on vacant land near the factories. Slag wastes deposited over the past 125 years cover approximately 31 square miles. They are the major fill material in the shallow groundwater aquifer. Therefore, the impact of these slag materials on the groundwater geochemistry and water quality around Lake Calumet is a major concern.

D. Groundwater chemistry in the Lake Calumet area

The stratigraphy of the Lake Calumet area consists of unconsolidated lake sediments and glacial tills overlying Silurian dolomite bedrock (Roadcap and Kelly, 1994a). The shallow aquifer in the area is the Equality Formation. The shallow aquifer also includes the man-made fill deposits covering most of the area (Roadcap and Kelly, 1994b). The Equality Formation is comprised of beach sands and lacustrine sands, silts, and clays deposited on the floor of Lake

Michigan during the post-glacial period. The deep aquifer in the area is confined to the dolomite bedrock which lies approximately 100 feet below ground surface.

The lithologic and hydrogeologic character of the fill is extremely heterogeneous. The fill material reaches a thickness of 10 feet in some areas. It is difficult to contour the fill thickness due to its haphazard disposal pattern. This may explain why groundwater chemistry is variable in the area.

The Illinois State Water Survey (ISWS) has been actively researching the migration and nature of contaminants throughout the Lake Calumet shallow groundwater system. The primary objective of the ISWS study is to obtain a regional picture of the groundwater chemistry because of the large number of contaminated sites and facilities which require remediation. To assist in these efforts, the ISWS has installed 21 monitoring wells since 1991 that cover the area around the lake (Figure 1). Periodic sampling is undertaken by the ISWS to assess the temporal variability of the water quality.

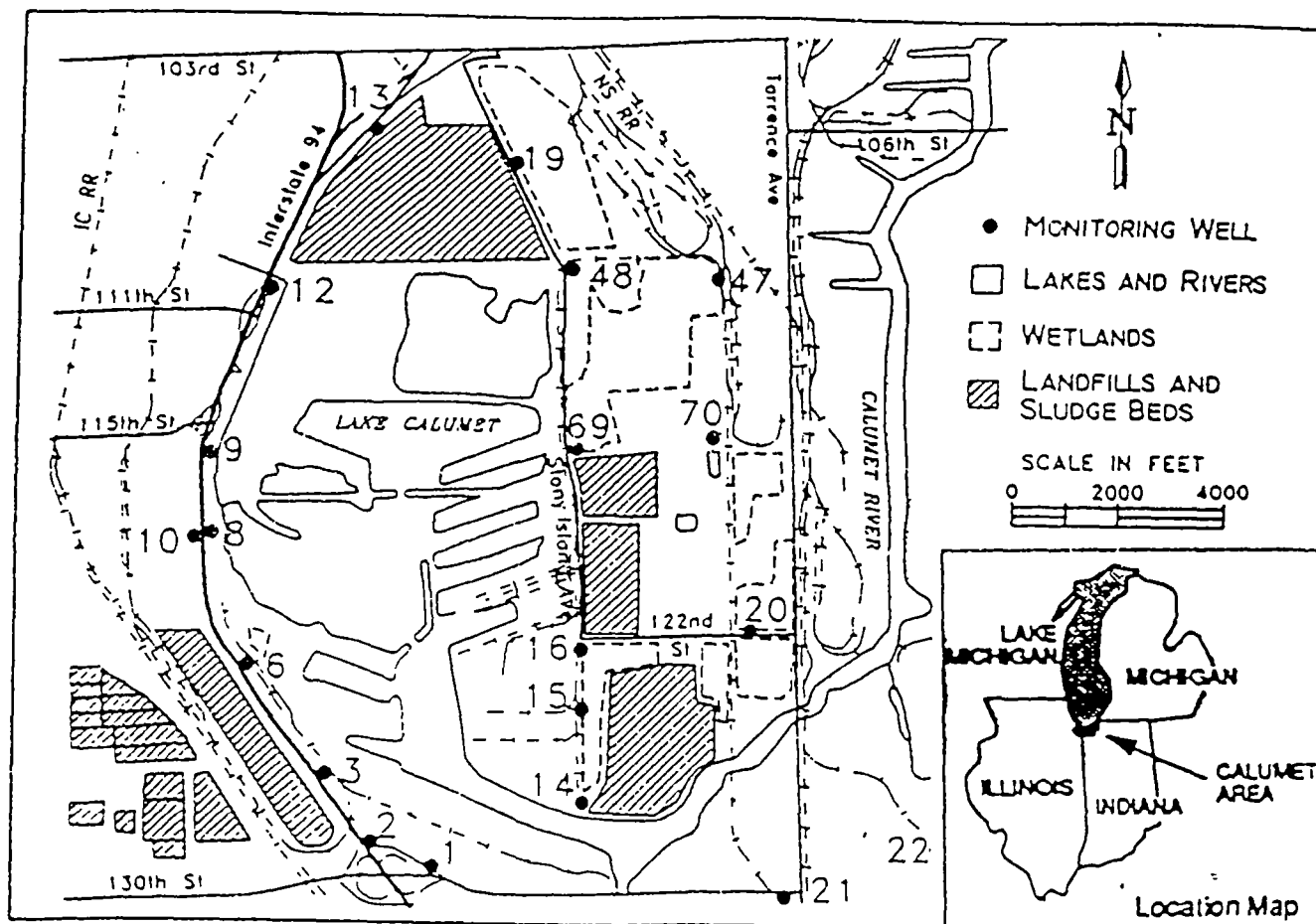


Figure 1 Study area map and locations of monitoring wells

(after Roadcap and Kelly, 1994)

Of particular interest in the context of the present study are ISWS monitoring wells #2, #3, and #70, where pH values in excess of 12 were recorded. According to the Resource Conservation and Recovery Act (RCRA) groundwater with a pH value higher than 12 is hazardous (Arguden, 1997, personal communication). These extremely high pH values are anomalous and are probably associated with pollution sources in the area. Table 1 lists the analytical results for groundwater samples from well #2 in the period 1991 to 1994. Figure 2 is the well log of well #2.

In addition to high pH values, elevated levels of organic and inorganic pollutants were identified in the water collected from the ISWS monitoring wells. Organic pollutants include dichloroethylene (DCE), benzene, toluene, and xylene (Roadcap and Kelly, 1994c). The water in these wells also contains relatively high concentrations of Ca, Na, Al, SO_4^{2-} , and Mo, but relatively low concentrations of Mg, Mn, Si, and Fe compared to the water of other wells in the Lake Calumet area. Inorganic contamination of the other ISWS wells include high levels of total dissolved solids (TDS), high concentrations of Fe, NH_4^+ , F^- , and heavy metals such as Ba, Cr, and Mn (Roadcap and Kelly, 1994d).

Roadcap and Kelly (1994e) proposed four possible sources of high pH in the groundwater system in the Lake Calumet area, namely fly ash deposits, liquid alkaline wastes, buried concrete, and steel mill slag. Leachate from fly ash usually has $\text{pH} > 10$ (Mattigod et al., 1990). The dissolution of concrete can produce a solution pH in excess of 12 (Berner, 1988). Liquid alkaline wastes can also account for high pH values.

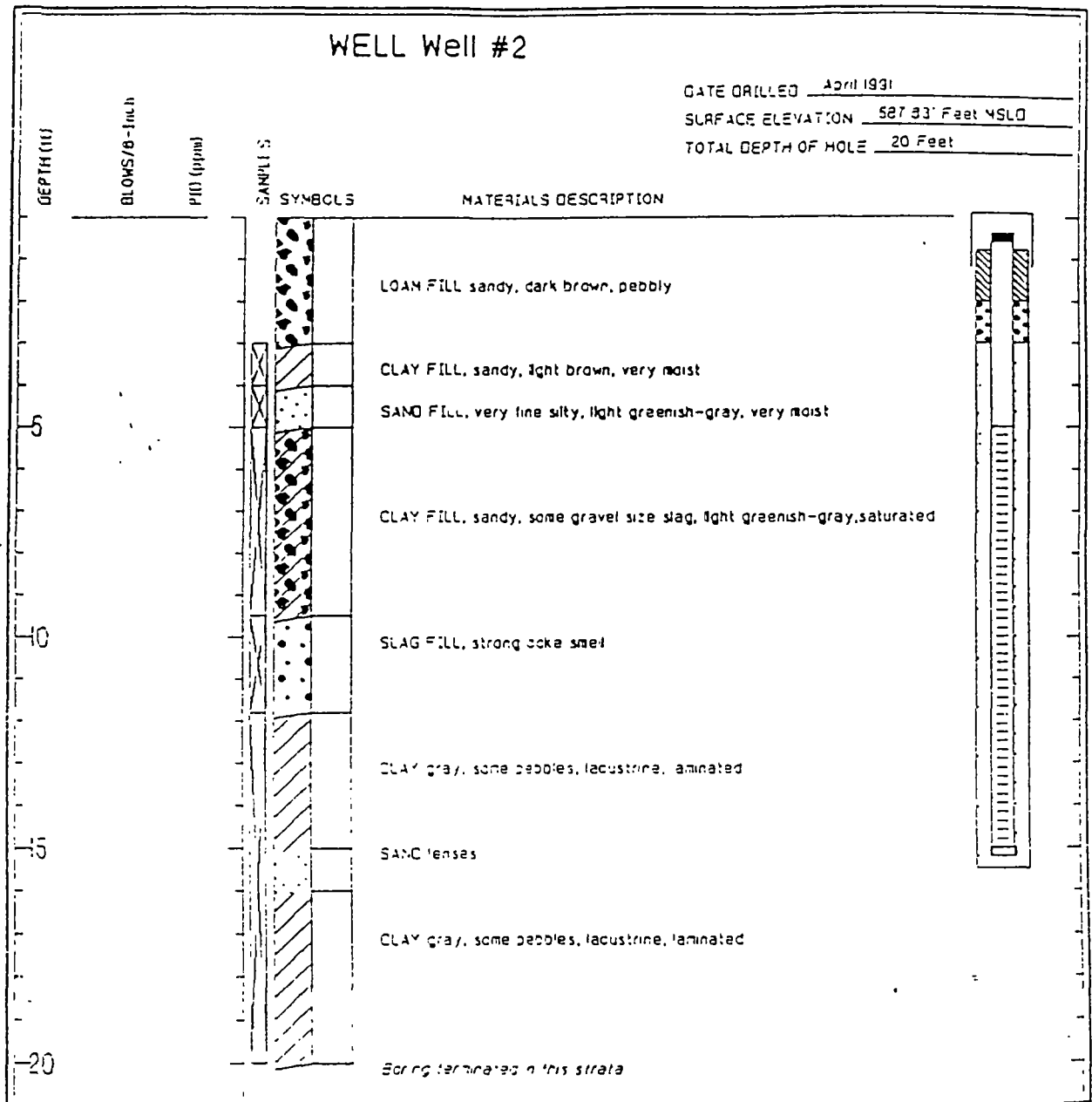


Figure 2 Well log of well #2

TABLE I
GROUNDWATER CHEMISTRY OF WELL #2 NEAR LAKE CALUMET

| Major (mg/L) | R1 ^a | R2 ^b | R3 ^c | R4 ^d | Average |
|---------------------|-----------------|-----------------|-----------------|-----------------|---------|
| Ca | 757 | 696 | 557 | 523 | 633 |
| Mg | 0.089 | 0.39 | 2.97 | 4.78 | 2.1 |
| Na | 2404 | 1950 | 2049 | 2414 | 2204 |
| K | 107 | 103 | 74.7 | 76.6 | 90 |
| Cl | 4102 | 4132 | 4460 | 5419 | 4528 |
| SO ₄ | 543 | 538 | 480 | 607 | 542 |
| Alkalinity | 696 | 474 | 438 | 206 | 453 |
| TDS | 7980 | 8849 | 7703 | 7683 | 8054 |
| TOC | 45 | 70 | 27 | | 35 |
| pH | 12 | 11.6 | 11.6 | 11.11 | 11.58 |
| Secondary (mg/L) | | | | | |
| NH ₄ | 25 | 33 | 28.75 | 19.9 | 26.67 |
| NO ₃ | <0.1 | 4.6 | <5 | | 4.6 |
| NO ₂ | <10 | | | | |
| PO ₄ | 0.7 | 1.8 | <5 | <0.08 | 1.25 |
| Al | 0.161 | 0.523 | 0.349 | 0.14 | 0.29 |
| B | 0.076 | | <0.13 | 0.184 | 0.13 |
| F | 3.2 | 2.9 | 2.9 | <1.5 | 3 |
| Fe | 0.078 | 0.091 | 0.083 | 0.104 | 0.09 |
| Mn | <0.002 | <0.002 | | <0.002 | |
| Si | 1.83 | <0.019 | 2.92 | 3.66 | 2.8 |
| Sr | 3.97 | 3.91 | 4.01 | 3.48 | 3.84 |
| Trace Metals (mg/L) | | | | | |
| Sb | <0.15 | <0.15 | <0.1 | <0.10 | |
| As | <0.08 | <0.08 | <0.04 | <0.04 | |
| Ba | 0.176 | 0.21 | 0.221 | 0.264 | 0.22 |
| Be | <0.001 | <0.001 | <0.002 | | |
| Cd | <0.006 | <0.006 | <0.004 | | |
| Cr | 0.009 | 0.011 | 0.007 | 0.006 | 0.008 |
| Co | <0.006 | <0.006 | 0.005 | <0.004 | 0.005 |
| Cu | <0.001 | <0.001 | <0.003 | 0.004 | 0.004 |
| Pb | <0.027 | <0.027 | <0.012 | | |
| Li | 0.382 | 0.219 | 0.191 | 0.229 | 0.25 |
| Hg | <0.03 | <0.03 | <0.02 | | |
| Mo | 0.349 | 0.391 | 0.36 | 0.466 | 0.39 |
| Ni | <0.018 | <0.018 | <0.006 | 0.014 | 0.01 |
| Se | <0.11 | <0.11 | <0.05 | | |
| Ag | <0.003 | <0.003 | <0.003 | | |
| Tl | <0.17 | <0.24 | <0.05 | <0.05 | |
| Sn | <0.06 | <0.06 | <0.04 | <0.04 | |
| Ti | 0.005 | 0.003 | 0.005 | 0.008 | 0.005 |
| V | <0.011 | <0.011 | 0.013 | 0.011 | 0.01 |
| Zn | <0.003 | <0.003 | <0.003 | <0.003 | |

^a May 91^b Sept 91^c June 92^d Sept 94

A number of researchers examined contamination in urban aquifers and found that industrial sites that process metals are significant point sources. Ford and Tellam (1994) found that elevated levels of total dissolved solids (TDS), sulfate, chloride, sodium, boron, and heavy metals were associated with metal working sites in Birmingham, UK. Ali (1992) also reported elevated levels of heavy metals in ground water near metal industries.

Doss (1996a) found significant enrichments in Na^+ , K^+ , Ca^{2+} , Fe^{2+} , Mg^{2+} , HCO_3^- , NH_4^+ , Cl^- , and SO_4^{2-} in waters that are hydraulically connected with steel-slag dumps in northwest Indiana. It is noteworthy that none of the wells sampled for the study by Doss were located within the steel-mill slag. The implication is that the ground water - slag interactions and their influences on water chemistry extend beyond the physical boundaries of disposed slag.

II. METHODS

A. Sampling of slag materials

1. Monitoring well

Samples used in this study were collected from a split spoon during the installation of well #2 in 1991 (Figure 2). The split spoon recovered the slag samples from a depth of 11.4 to 11.8 feet below ground surface at which depth, according to the well log data, the bulk of the slag material is located. The groundwater table is about four to five feet below ground surface and covers the slag material. The size of the samples ranged from pebble to sand grains.

Five samples (sample ID's S1, S2, S3, S4, and S5) the size of small pebbles as shown in Figure 3, were selected to be representative. These samples represent the significant heterogeneity of observed slag material. However, it is not assumed or expected that these samples represent the entire population of disposed slag in the area. Much more intensive sampling throughout the body of the disposed slag would be required for such characterization. The collected samples do however provide insight into the nature of the slag that occurs in the study area. The exact slag burial date is not known, but is believed to have been before 1920 (Roadcap, 1996, personal communication).

The steel slag samples were separated from the surrounding material of sandy clay. Samples were sonically cleaned to remove loose deposits from the surface. Each slag "pebble" was cut in half to make a thin section and the remaining material was pulverized for use in X-ray diffraction and leaching experiments.

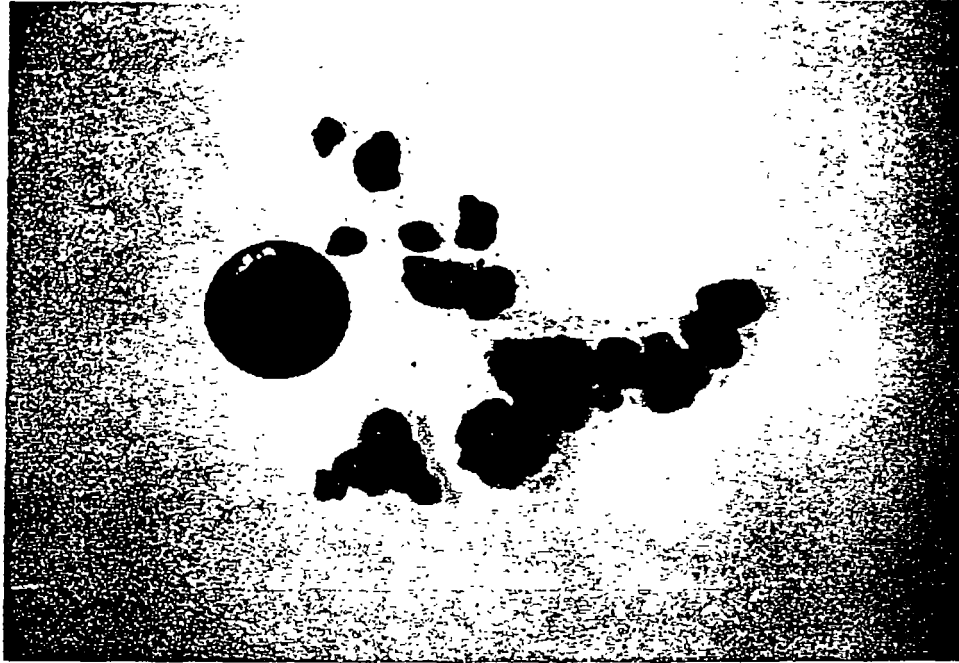


Figure 3 Field samples of steel slag used in the study A penny (19 mm diameter) is shown for scale

2. Slag piles

Blastfurnace slag represents the other major category of steel mill slags. Fresh blastfurnace slag was collected from Koch Materials, Inc in Indiana. Koch Materials manages the huge quantities of blastfurnace slag generating from a nearby United States Steel (USS) plant. Figure 4 shows the blastfurnace slag samples used in the study. Figure 5 is a photo portraying the vast amounts of blastfurnace slag generated from USS.

Fresh blastfurnace slag was investigated in this study because it was not subject to weathering, in contrast to the field samples collected in Lake Calumet monitoring wells. The objective was to determine the effects of blastfurnace slag leachates to surface and groundwater chemistry, considering the wide variety of its uses. Blastfurnace slag is used in highway construction, railroad ballasts, cement and concrete aggregate, raw material for Portland cement, mineral wool, and cinder block (Lewis, 1993). It is also used in wastewater treatment as a material for septic-tank absorption beds and as a biological filter media. If the slag is ground finely, it can be added to soil to make it alkaline (Nemerow, 1984).



Figure 4 Blastfurnace slag samples used in the study Ball-point pen (15 cm long) shown for scale



Figure 5 Blastfurnace slag piles at Koch Materials Inc in Indiana

B. Characterization of slags

1. X-ray diffraction

X-ray Diffraction (XRD) analysis was performed with a Siemens D-5000 powder diffractometer using Cu radiation to identify crystalline phases present in steel and blastfurnace slag samples. An understanding of the “mineral” phases present in the slag samples and their chemical compositions is needed for interpreting the results of the batch powder-reaction tests. The steel slag samples from well #2 exhibited an outer weathered part and an unweathered core. Separation of the outer weathered part from the unweathered core was done using an engraving tool, for two samples, S3 and S5. The weathered and unweathered parts were analyzed separately

2. Optical and electron microscopy

Thin sections were prepared from slag samples. The weathered parts of the steel slag samples were softer and more friable than the core part, so some weathered material was lost during polishing. A polarizing light microscope was used to identify phases present in the slag samples. A scanning electron microscope (SEM) was used to measure the chemical compositions of the slag samples. The SEM used in this study was a JEOL JSM-35CF model coupled with a Tracor Northern 5500 Energy Dispersive System (EDS) X-ray microanalyzer to perform semi-quantitative elemental analyses. Conventional Bence-Albee correction procedures were used for chemical analyses. The Back Scattered Electron image (BEI) mode, which identifies contrasts in elemental composition according to atomic number (Z), was used for imaging the sample's surface

C. Batch powder-reaction experiments

1. Steel slag samples

The purpose of the batch powder-reaction experiments was to correlate the steel slag leachate chemistry with the existing groundwater chemistry in well #2, to investigate variations in the solution pH, and to investigate the potential mobilization of heavy metals. A leaching test provides information of the components that are likely to be released from a waste, an indication of their maximum concentrations in the leachate, and the total amount to be released per unit weight of waste (Ham et al., 1979a). Because the groundwater environments in the study area is reducing, the leaching experiments for the steel slag samples were conducted under anoxic conditions.

The core parts of samples S3 and S4 were selected for leaching experiments because they were least affected by weathering. The leaching experiments were conducted at room temperatures (22-23° C). Sample S3 was mixed with dilute 0.1 M HNO₃ and sample S4 was mixed with Milli-Q ultra pure water. The water and the HNO₃ were degassed before mixing with the steel slag to remove dissolved atmospheric gases. Approximately 50 ml of solution + solid was placed in airtight bottles to keep atmospheric gases from entering into the solutions. The bottles were then placed in a shakerbath for a period of one month.

The reason for using dilute acid was to simulate an actively decomposing landfill where low pH leachates might react with steel slag. In this case, the release of constituents that are found in the steel slag sample could be greatly enhanced. The pH of distilled water is close to the pH of a normal rain water.

2. Blastfurnace slag samples

The blastfurnace slag samples collected from Koch Materials, Inc. were in the size range of large pebbles (5 - 10 cm in diameter) and were ground and sieved to provide a uniform small grain size (63 to 125 μm). The specific surface area of the slag powder was 0.39 m^2/g , measured with the N_2 -BET method

A solid to water mass ratio of 16:1 was used, in accordance with EPA method 1310 (USEPA, 1986). This procedure is commonly used to simulate leaching of waste in a sanitary landfill. The leaching media used for this study was dilute nitric acid at various concentrations. Milli-Q ultra pure water has a pH of six and was part of the leaching test series. The leaching media correspond to liquids likely to be in contact with the waste in the landfill. Acid leaching media can therefore simulate an actively decomposing landfill, whereas distilled water represents a more stabilized landfill

Two sets of leaching experiments were performed. The first one was performed under oxic conditions with solutions open to atmospheric air, and the second was performed under Ar gas to create anoxic conditions. Five (5.00) g of slag was used with approximately 80 g of solution. A magnetic stirrer was used throughout the experiment. After 24 hours the pH was measured and each leachate solution was filtered with a 0.45 micron filter and submitted for analysis.

The temperature of the experiment was kept constant at room temperature (22 - 23° C for the oxic series and 14 - 15° C for the anoxic series). These temperatures resemble the ones at the land surface (for the oxic experiments) and in the subsurface (anoxic conditions in contact with

cooler groundwater) Six leachant solutions were used for each of the leaching experiments. These solutions were dilute HNO_3 having different pH values (Table 2).

TABLE II
INITIAL pH OF BLASTFURNACE SLAG LEACHATES
(OXIC AND ANOXIC SERIES)

| Leachate ^b | pH ^a | Leachate ^c | pH |
|-----------------------|-----------------|-----------------------|------|
| OFSL-1 | 1.15 | AFSL-1 | 1.4 |
| OFSL-2 | 2.04 | AFSL-2 | 2 |
| OFSL-3 | 3.1 | AFSL-3 | 2.94 |
| OFSL-4 | 3.95 | AFSL-4 | 3.88 |
| OFSL-5 | 5.02 | AFSL-5 | 5.05 |
| OFSL-6 | 5.98 | AFSL-6 | 5.82 |

^a pH units

^b Oxic

^c Anoxic

III. RESULTS

A. Steel slag from Lake Calumet well #2

1. X-ray diffraction results

Table 3 gives relative intensities of observed diffraction peaks for the steel slag samples, along with corresponding d-spacings. The best-fit mineral phases matching these d-spacings, according to data from the Joint Commission of Powder Diffraction Society (JCPDS) files, are also shown in Table 3.

“Bredigite” , “rankinite”, “merwinite”, “monticellite”, “wustite”, and “larnite” were identified, based on XRD analysis in the core parts of the field samples. These are typical crystalline phases found in slag materials and can occur in any combination. The weathered parts consisted of four crystalline phases : “calcite”, “dolomite”, “wustite”, and “quartz”.

The core parts yielded low intensity peaks suggesting the glassy nature of the slag samples. The peaks were sharp enough to be easily identified, however, indicating that there are well crystallized “minerals” in the steel slag samples. The weathered parts had much higher and more well-defined peaks.

It is noteworthy that the phases present in the steel slag samples have extensive substitution from other elements namely Fe and Mn in their structure. “Monticellite” from sample S4 has up to 9 % and 10 % by weight of MnO and FeO respectively substituting for MgO in its structure. These substitutions distort the crystal lattice resulting in a shift of the peaks in the X-ray pattern.

TABLE III
d SPACING AND RELATIVE INTENSITIES OF STEEL SLAG SAMPLES

| JCPDS Files | | | S1 | | S2 | | JCPDS files | | | S3 | | S4 | | S5 | | | | | | | | | | |
|-------------------|---------|--------------|--------------|---|------|---------|--|---------|--------------|------|---------|------|---------|------|---------|--|--|--|--|--|--|--|--|--|
| d Å | Rel I % | Phases | d Å | Rel I % | d Å | Rel I % | d Å | Rel I % | Phase | d Å | Rel I % | d Å | Rel I % | d Å | Rel I % | | | | | | | | | |
| 2.69 | 100 | Merwinite | 2.68 | 100 | 2.68 | 77 | 2.69 | 100 | Merwinite | --- | --- | 2.69 | 100 | --- | --- | | | | | | | | | |
| 2.67 | 65 | Merwinite | --- | --- | --- | --- | 2.67 | 65 | Merwinite | --- | --- | 2.70 | 59 | --- | --- | | | | | | | | | |
| 2.65 | 47 | Merwinite | --- | --- | --- | --- | 2.65 | 47 | Merwinite | --- | --- | --- | --- | --- | --- | | | | | | | | | |
| 1.91 | 35 | Merwinite | --- | --- | --- | --- | 1.91 | 35 | Merwinite | --- | --- | --- | --- | --- | --- | | | | | | | | | |
| 2.76 | 26 | Merwinite | --- | --- | --- | --- | 2.76 | 26 | Merwinite | --- | --- | --- | --- | --- | --- | | | | | | | | | |
| 2.66 | 100 | Monticellite | --- | --- | --- | --- | 2.78 | 100 | Larnite | 2.75 | 79 | 2.95 | 62 | 2.75 | 100 | | | | | | | | | |
| 1.82 | 60 | Monticellite | 1.83 | 57 | --- | --- | 2.79 | 97 | Larnite | 2.81 | 32 | 2.85 | 34 | 2.78 | 46 | | | | | | | | | |
| 2.58 | 59 | Monticellite | --- | --- | --- | --- | 2.74 | 83 | Larnite | --- | --- | --- | --- | --- | --- | | | | | | | | | |
| 3.63 | 51 | Monticellite | --- | --- | --- | --- | 2.19 | 51 | Larnite | 2.18 | 50 | --- | --- | 2.16 | 21 | | | | | | | | | |
| 2.93 | 44 | Monticellite | --- | --- | --- | --- | 2.61 | 42 | Larnite | 2.61 | 38 | 2.61 | 51 | 2.61 | 25 | | | | | | | | | |
| 2.40 | 29 | Monticellite | 2.41 | 40 | --- | --- | 2.72 | 30 | Larnite | 2.71 | 37 | --- | --- | 2.73 | 22 | | | | | | | | | |
| 1.59 | 27 | Monticellite | 1.60 | 32 | --- | --- | 1.98 | 24 | Larnite | --- | --- | --- | --- | 1.98 | 21 | | | | | | | | | |
| 3.02 | 100 | Rankinite | --- | --- | 3.04 | 70 | 2.15 | 100 | Wustite | 2.16 | 100 | --- | --- | 2.15 | 55 | | | | | | | | | |
| 2.72 | 80 | Rankinite | --- | --- | --- | --- | --- | --- | --- | --- | --- | --- | --- | 2.14 | 31 | | | | | | | | | |
| 2.91 | 60 | Rankinite | 2.95 | 73 | --- | --- | 2.49 | 80 | Wustite | 2.49 | 53 | --- | --- | --- | --- | | | | | | | | | |
| 3.84 | 50 | Rankinite | 3.87 | 29 | --- | --- | 1.52 | 60 | Wustite | 1.52 | 38 | --- | --- | --- | --- | | | | | | | | | |
| 3.79 | 50 | Rankinite | 3.66 | 70 | --- | --- | 1.30 | 25 | Wustite | --- | --- | --- | --- | --- | --- | | | | | | | | | |
| 4.49 | 30 | Rankinite | --- | --- | 4.55 | 29 | 2.66 | 100 | Monticellite | 2.62 | 32 | 2.62 | 46 | --- | --- | | | | | | | | | |
| 2.59 | 30 | Rankinite | 2.60 | 59 | 2.51 | 32 | 1.82 | 60 | Monticellite | 1.76 | 36 | 1.84 | 54 | --- | --- | | | | | | | | | |
| 3.34 | 100 | Quartz | 3.35 | 55 | 3.35 | 100 | 2.58 | 59 | Monticellite | --- | --- | --- | --- | --- | --- | | | | | | | | | |
| 4.26 | 22 | Quartz | 4.26 | 22 | 4.26 | 29 | 3.63 | 51 | Monticellite | --- | --- | 3.67 | 45.4 | --- | --- | | | | | | | | | |
| --- | --- | --- | --- | --- | 4.22 | 34 | 2.93 | 44 | Monticellite | --- | --- | --- | --- | --- | --- | | | | | | | | | |
| --- | --- | --- | --- | --- | --- | --- | 2.4 | 29 | Monticellite | --- | --- | 2.42 | 32.7 | --- | --- | | | | | | | | | |
| --- | --- | --- | --- | --- | --- | --- | --- | --- | --- | --- | --- | 2.09 | 27 | --- | --- | | | | | | | | | |
| 1.82 | 14 | Quartz | --- | --- | --- | --- | Phases identified : Larnite Wustite Monticellite | | | | | | | | | | | | | | | | | |
| 2.15 | 100 | Wustite | 2.14 | 25 | 2.17 | 70 | | | | | | | | | | | | | | | | | | |
| --- | --- | --- | --- | --- | 2.16 | 47 | | | | | | | | | | | | | | | | | | |
| 2.49 | 80 | Wustite | --- | --- | --- | --- | Merwinite Larnite Monticellite | | | | | | | | | | | | | | | | | |
| 1.52 | 60 | Wustite | --- | --- | --- | --- | | | | | | | | | | | | | | | | | | |
| 1.3 | 25 | Wustite | --- | --- | --- | --- | | | | | | | | | | | | | | | | | | |
| --- | --- | --- | 5.58 | 32 | 9.82 | 29 | Larnite Wustite | | | | | | | | | | | | | | | | | |
| Phases identified | | | Merwinite | Merwinite Rankinite Quartz Wustite | | | | | | | | | | | | | | | | | | | | |
| | | | Monticellite | | | | | | | | | | | | | | | | | | | | | |
| | | | Rankinite | | | | | | | | | | | | | | | | | | | | | |
| | | | Quartz | | | | | | | | | | | | | | | | | | | | | |
| | | | Wustite | | | | | | | | | | | | | | | | | | | | | |

*** : Peak expected but not identified in sample
--- : Peak absent

--- : Peak expected but not identified in sample

--- : Peak absent

TABLE III (continued)

d SPACING AND RELATIVE INTENSITIES OF STEEL SLAG SAMPLES

| JCPDS file | | | S3 weathered | | S5 weathered | |
|---------------------|---------|----------|--------------|---------|--------------|---------|
| d Å | Rel I % | phase | d Å | Rel I % | d Å | Rel I % |
| 3.34 | 100 | Quartz | 3.34 | 100 | 3.34 | 100 |
| 4.26 | 22 | Quartz | 4.26 | 29 | 4.26 | 18 |
| | | | 4.29 | 27 | | |
| 1.82 | 14 | Quartz | *** | *** | *** | *** |
| 3.03 | 100 | Calcite | 3.04 | 44 | 3.04 | 46 |
| 1.87 | 34 | Calcite | 1.91 | 17 | *** | *** |
| 3.85 | 29 | Calcite | 3.86 | 21 | *** | *** |
| 2.09 | 27 | Calcite | *** | *** | 2.09 | 12 |
| 2.28 | 18 | Calcite | *** | *** | 2.28 | 13 |
| 2.89 | 100 | Dolomite | 2.89 | 32 | 2.89 | 23 |
| 1.79 | 30 | Dolomite | 1.80 | 19 | *** | *** |
| 1.78 | 30 | Dolomite | *** | *** | *** | *** |
| 2.19 | 30 | Dolomite | *** | *** | *** | *** |
| 2.15 | 100 | Wustite | *** | *** | 2.15 | 15 |
| 2.49 | 80 | Wustite | 2.49 | 21 | 2.49 | 11 |
| 1.52 | 60 | Wustite | *** | *** | 1.52 | 11 |
| 1.30 | 25 | Wustite | *** | *** | *** | *** |
| --- | --- | --- | 2.65 | 26 | | |
| phases identified : | | | Quartz | | Quartz | |
| | | | Calcite | | Calcite | |
| | | | Dolomite | | Dolomite | |
| | | | Wustite | | Wustite | |

*** : Peak expected but not identified in sample

--- : Peak absent

2. Optical and electron microscopy results

SEM/EDS analysis yielded sharp chemical differences within the steel slag samples. The outside weathered part can be clearly identified. Photographs of light microscope and electron microscope images of selected areas were taken to demonstrate these differences. Characteristic dendritic features were prominent in the steel slag samples. Figure 6 is a photomicrograph taken with the light microscope (transmitted light) of a selected area of sample S1. Figure 7 shows the same area viewed under the SEM with the back scattered image mode.

SEM/EDS analysis revealed that the dendrites are Fe-Mn rich areas. Photomicrographs of thin sections of slag from Derge (1964) showed these dark colored dendrites to be $(\text{Fe,Mn})_3\text{O}_4$ embedded into a lighter phase described as $(\text{Ca, Mg, Mn, Fe})_2\text{SiO}_4$. This is similar to CaMgSiO_4 (monticellite), identified from XRD and confirmed by SEM/EDS analysis in the samples of this study. CaMgSiO_4 is a typical crystalline phase in the slag samples that can also include Fe and Mn in its structure.

The back scattered image mode of the SEM revealed lower brightness of the outside weathered part as compared to the core part. This indicated the dominance of elements with low atomic numbers such as Ca, Si, and Al. However, Ca has a relatively higher atomic number but it is present in carbonates (CaCO_3) therefore lowering the overall brightness of the image. Areas with increased brightness in the core part indicated the presence of elements with higher atomic numbers such as Fe and Mn. The high concentrations of Fe and Mn and the presence of metallic iron (representing droplets of liquid iron entrained in the slag) suggest that the field samples are steel slag instead of blastfurnace slag.

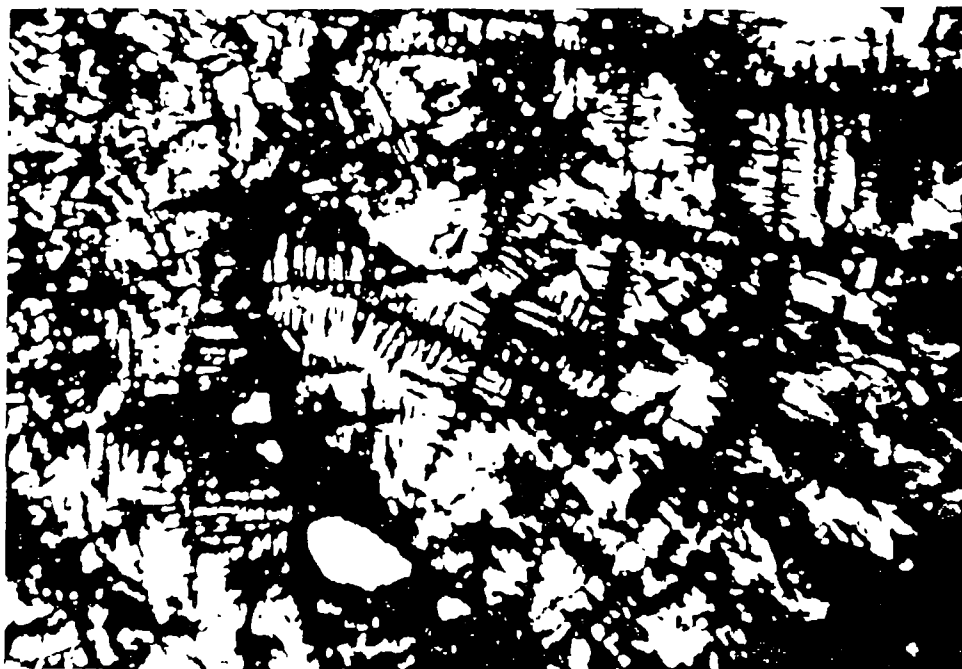


Figure 6 Photomicrograph of sample S1 viewed under the light microscope (transmitted light)

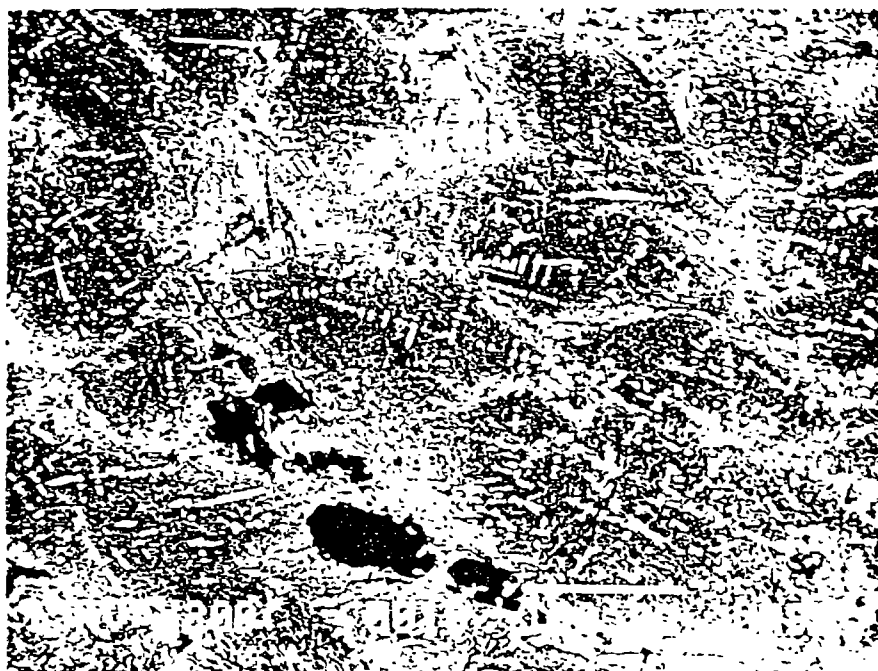


Figure 7 Photomicrograph of the same area under the SEM (BEI mode)

According to SEM/EDS analysis (Table 4), FeS_2 was detected in the weathered part of sample S5 (Figure 8) and in the material surrounding the steel slag samples (Figure 9). Presumably it corresponds to “pyrite” crystals. Pyrite is a secondary mineral that forms under reducing conditions. The “pyrite” crystals have a relatively euhedral shape (Figure 8). The source of Fe and S are likely from the sample itself since Fe and S are present in the core part of the samples. It is also possible that some of the Fe and S could be from outside the slag. In either case, the presence of pyrite reveals reducing conditions during the weathering of these slag materials.

“Wustite” (FeO) and “rutile” (TiO_2) were detected in the weathered part of sample S4. These phases are relatively resistant to weathering and they are the remainders from the weathering process that transformed the initial slag components to the phases that constitute the weathered part.

SEM/EDS analysis of certain selected points of the core part of samples S3 and S4 indicated the presence of high concentrations of Si, Fe, Mn, Mg, and Ca. The concentration of Al is relatively lower. Elements like Ti, Na, Cr, S and P were detected in trace amounts. Sample S3 had numerous steel droplets trapped in the slag structure. SEM/EDS analyses for samples S3 and S4 are summarized in Tables 5 and 6 respectively. SEM photomicrographs of samples S3 and S4 are shown in Figures 10 and 11 respectively.

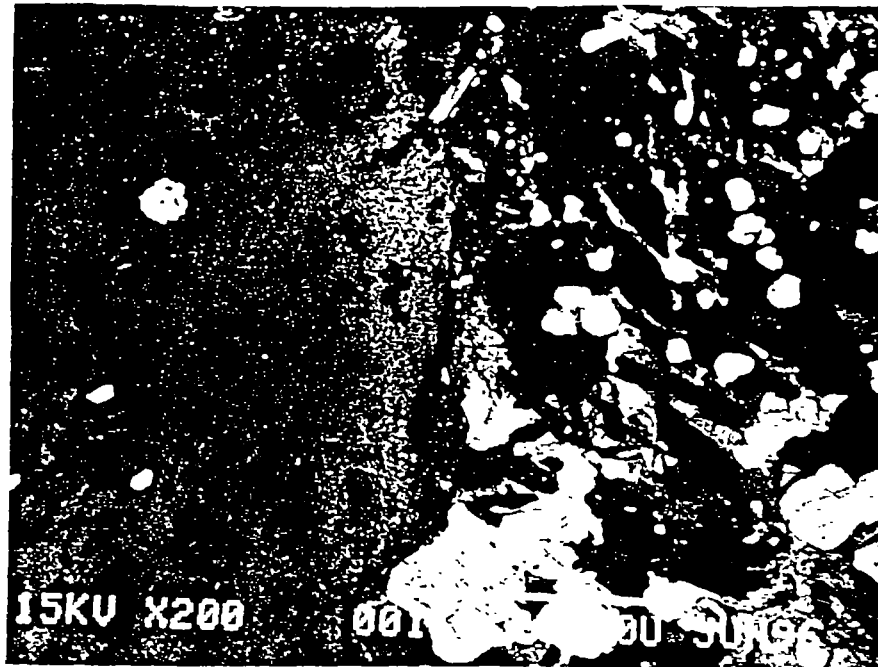


Figure 8 SEM photographs (BEI mode) showing microcrystalline "pyrite" embedded in the weathered part of steel slag S5

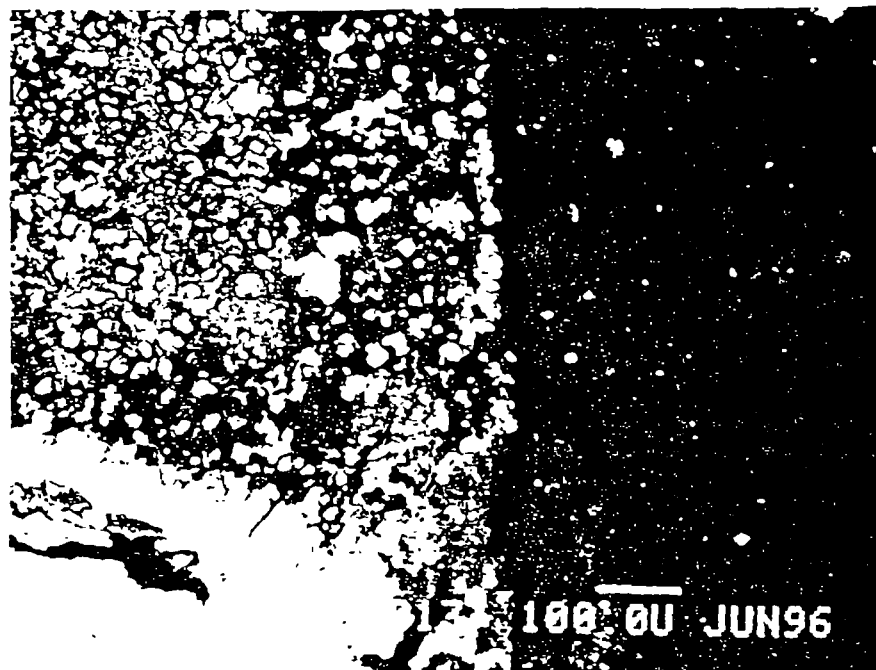


Figure 9 SEM photograph showing "pyrite" (FeS_2) crystals in the core sample SSA where steel slag was buried

The steel slag samples were mostly glassy, especially for sample S1, and display a relatively porous structure. Samples S1, S2, S3, and S4 exhibited microcrystalline phases presumably caused by rapid cooling of the slag. Sample S5 has relatively larger crystals, mainly β' - Ca_2SiO_4 (larnite) and FeO (wustite). "Larnite" typically occurs in slags. Larger crystals suggest a slower cooling rate. "Wustite" does not commonly occur in nature and is usually opaque to transmitted light. It occurs only in steel mill slags and meteorites.

The outer weathered skin of all samples as viewed under the light microscope appeared to be mostly tiny crystals of calcite with some large quartz, dolomite and clay minerals. Calcite was found to be associated with vesicular pores in the structure of slag.

TABLE IV

SEM/EDS ANALYSIS OF FeS_2 IN SAMPLE S5

| OXIDE | NORM'D WT % | CALC'D WT % |
|-------------------------|-------------|-------------|
| SiO_2 | 0.25 | 0.46 |
| TiO_2 | 0.00 | 0.00 |
| Al_2O_3 | 0.00 | 0.00 |
| FeO | 30.19 | 55.31 |
| MnO | 0.00 | 0.00 |
| MgO | 0.07 | 0.12 |
| CaO | 0.25 | 0.45 |
| Na_2O | 0.24 | 0.44 |
| K_2O | 0.00 | 0.00 |
| Cr_2O_3 | 0.08 | 0.15 |
| NiO | 0.00 | 0.00 |
| SO_3 | 68.92 | 126.28 |
| Total : | 100 | 183.22 |

TABLE V

SEM/EDS ANALYSIS OF THE CORE PART OF FIELD SAMPLE S3

| CALC'D WT % | S3-B | S3-C | S3-D | S3-E | S3-H | S3-J | Average |
|--------------------------------|-------|-------|-------|-------|--------|-------|---------|
| SiO ₂ | 0.74 | 0.64 | 31.44 | 32.38 | 0.47 | 49.05 | 19.12 |
| TiO ₂ | 1.96 | 0.58 | 0 | 0.16 | 0 | 0.39 | 0.51 |
| Al ₂ O ₃ | 2.5 | 0.77 | 0.14 | 0 | 0.21 | 2.48 | 1.02 |
| FeO | 78.4 | 79.75 | 20.17 | 21.92 | 39.94 | 5.09 | 40.88 |
| MnO | 8.02 | 9.2 | 11.19 | 11.97 | 23.06 | 4.62 | 11.34 |
| MgO | 1.96 | 2.56 | 7.78 | 8.04 | 30.99 | 1.86 | 8.86 |
| CaO | 0.52 | 0.61 | 24.82 | 22.91 | 2.66 | 12.99 | 10.75 |
| Na ₂ O | 0.51 | 0 | 0.29 | 0.27 | 1.19 | 0.38 | 0.44 |
| K ₂ O | 0 | 0 | 0 | 0 | 0 | 0.33 | 0.05 |
| Cr ₂ O ₃ | 1.43 | 0.72 | 0.27 | 0.09 | 1.93 | 0.11 | 0.76 |
| NiO | 0 | 0 | 0 | 0 | 0 | 0 | 0 |
| SO ₃ | 0 | 0 | 0 | 0 | 0 | 0.42 | 0.07 |
| P ₂ O ₅ | 0 | 0 | 0 | 0 | 0 | 0 | 0 |
| Total | 96.04 | 94.82 | 96.11 | 97.74 | 100.45 | 77.72 | 93.18 |

SEM/EDS ANALYSIS OF THE WEATHERED PART OF FIELD SAMPLE S3

| CALC'D WT % | S3-F | S3-G | S3-I | Average |
|--------------------------------|-------|-------|-------|---------|
| SiO ₂ | 0.23 | 38.97 | 36.21 | 25.14 |
| TiO ₂ | 0 | 0.07 | 0 | 0.07 |
| Al ₂ O ₃ | 0 | 4.63 | 11.66 | 8.14 |
| FeO | 0.15 | 8.53 | 0.09 | 2.92 |
| MnO | 0.93 | 1.91 | 0 | 1.42 |
| MgO | 4.65 | 14.38 | 8.8 | 9.28 |
| CaO | 50.91 | 6.03 | 38.59 | 31.84 |
| Na ₂ O | 0 | 0.37 | 0.23 | 0.30 |
| K ₂ O | 0 | 0 | 0.17 | 0.17 |
| Cr ₂ O ₃ | 0 | 0 | 0 | 0 |
| NiO | 0 | 0 | 0 | 0 |
| SO ₃ | 0.95 | 1.31 | 0.76 | 1.01 |
| P ₂ O ₅ | 0 | 0 | 0 | 0 |
| Total | 57.8 | 76.19 | 96.51 | 76.83 |

TABLE VI

SEM/EDS ANALYSES OF THE CORE PART OF FIELD SAMPLE S4

| CALC'D WT % | S4-A | S4-B | S4-C | S4-D | S4-G | S4-N | Average |
|--------------------------------|--------|--------|-------|-------|-------|-------|---------|
| SiO ₂ | 0.65 | 0.77 | 0.66 | 0.78 | 32.01 | 32.36 | 11.21 |
| TiO ₂ | 0 | 0 | 0 | 0 | 0.38 | 0.3 | 0.34 |
| Al ₂ O ₃ | 0.22 | 0.25 | 0 | 0.18 | 0 | 0 | 0.22 |
| FeO | 122.72 | 122.75 | 76.04 | 79.31 | 7.54 | 9.89 | 69.71 |
| MnO | 0.17 | 0.23 | 9.03 | 0.38 | 10.84 | 8.86 | 4.92 |
| MgO | 0.11 | 0 | 6.05 | 0.16 | 10.82 | 9.04 | 5.24 |
| CaO | 0 | 0.11 | 0.21 | 0.35 | 31.03 | 32.45 | 12.83 |
| Na ₂ O | 0.33 | 0.52 | 0.41 | 0.39 | 0 | 0 | 0.41 |
| K ₂ O | 0 | 0 | 0 | 0 | 0 | 0 | 0.00 |
| Cr ₂ O ₃ | 0 | 0 | 0.51 | 0.1 | 0.21 | 0.13 | 0.24 |
| NiO | 0 | 0 | 0 | 0 | 0 | 0 | 0.00 |
| SO ₃ | 0 | 0 | 0 | 0 | 0.23 | 0 | 0.23 |
| P ₂ O ₅ | 0 | 0 | 0 | 0 | 0 | 0 | 0.00 |
| Total | 124.2 | 124.63 | 92.9 | 81.64 | 93.06 | 93.04 | 101.58 |

SEM/EDS ANALYSES OF THE WEATHERED PART OF FIELD SAMPLE S4

| CALC'D WT % | S4-F | S4-I | S4-J | S4-K | S4-L | Average |
|--------------------------------|-------|-------|-------|-------|-------|---------|
| SiO ₂ | 0.37 | 0.26 | 0.46 | 0.68 | 56.53 | 11.66 |
| TiO ₂ | 0 | 0 | 0.08 | 0 | 0 | 0.08 |
| Al ₂ O ₃ | 0.16 | 0 | 0 | 0.18 | 15.69 | 5.34 |
| FeO | 0.31 | 0 | 2.9 | 0.52 | 0.82 | 1.14 |
| MnO | 0.11 | 0 | 0.17 | 0.19 | 0 | 0.16 |
| MgO | 16.13 | 0.56 | 15.75 | 0.19 | 0 | 8.16 |
| CaO | 30.56 | 48.94 | 29.11 | 49.05 | 0.39 | 31.61 |
| Na ₂ O | 0 | 0 | 0.44 | 0 | 0.43 | 0.43 |
| K ₂ O | 0 | 0 | 0 | 0.15 | 14.12 | 7.13 |
| Cr ₂ O ₃ | 0 | 0 | 0.11 | 0 | 0 | 0.11 |
| NiO | 0 | 0 | 0.08 | 0.25 | 0.09 | 0.14 |
| SO ₃ | 0.22 | 0.16 | 0.1 | 2.7 | 0 | 0.79 |
| P ₂ O ₅ | 0 | 0 | 0 | 0 | 0 | 0 |
| Total | 47.88 | 49.92 | 49.2 | 53.91 | 88.07 | 57.80 |

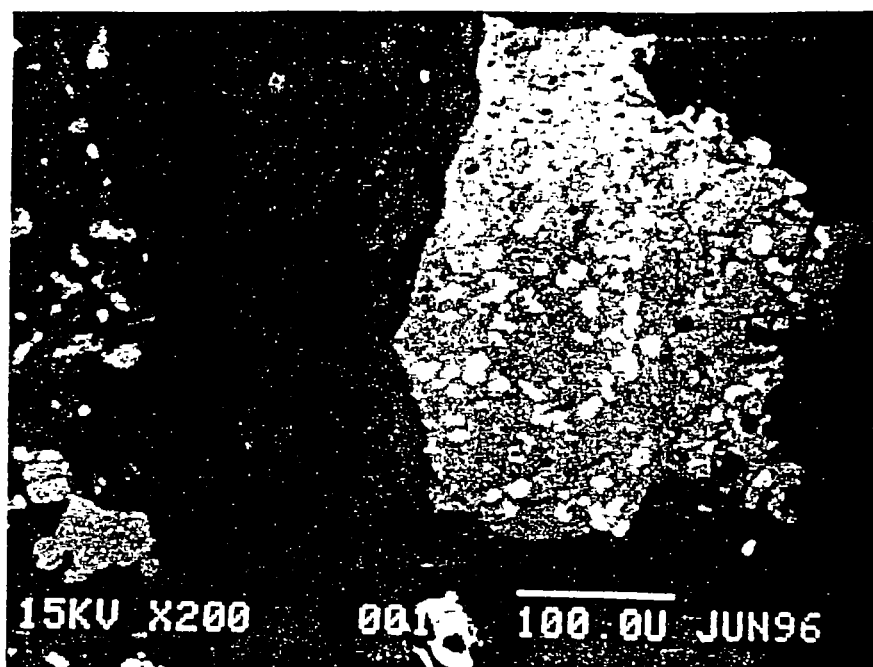


Figure 10 SEM photograph (BEI mode) of field sample S3



Figure 11 SEM photograph (BEI mode) of field sample S4

3. Batch powder-reaction results

Steel slag samples S3 and S4 were selected since they were examined with the SEM/EDS and XRD. The pH of the solution mixed with sample S3 was found to be 1.65 (pH units). 0.1015 g of S3 was added to 42.05 g of acid. With such a small amount of sample available, the solid to water ratio was low, approximately 1:415. The pH of the distilled water mixed with sample S4 was 5.6 (pH units). 0.2640 g of the sample was mixed with 42.10 g of the solution resulting in a solid to water ratio of approximately 1:160.

The pH of the final solution after one month in the shakerbath was measured to be 1.7 for leachate of sample S3 and 10.74 for the leachate of sample S4. The steel slag samples have the ability to increase the pH of the initial solution as demonstrated from the leachate of sample S4. Only 0.264 g of the solid sample was enough to increase the pH of the solution from 5.6 to 10.7. Despite the alkaline character of the steel slag, the relatively small amounts of S3 and the initial low pH of the solution kept the pH of the leachate low.

Analyses for metals in the steel slag leachates were conducted at the laboratories of the ISWS using inductively-coupled plasma emission spectroscopy (ICP). The samples (Table 7) were analyzed for Ca, Mg, Si, Al, Mn, Na, Sr, Ba, V, Cr, Cu, Fe, P, S, Ti, Zn, Be, Mo, Sn, Cl, NO₃-N, SO₄, and F. A number of elements were not detected in both the leachates. These are K, As, B, Cd, Pb, Hg, Ni, Se, Ag, Co, Li, Sb, Tl, Bi, NO₂-N, and PO₄-P.

TABLE VII
CHEMICAL ANALYSES OF FIELD SAMPLE
LEACHATES ^a

| Element | S3 | S4 |
|--------------------|-------|-------|
| Ca | 739 | 35 |
| Mg | 144 | 0.11 |
| Si | 132 | 13 |
| Al | 27 | ND |
| Mn | 129 | ND |
| Na | 2.86 | 1.22 |
| Sr | 0.47 | 0.06 |
| Ba | 0.32 | 0.11 |
| V | 0.73 | 0.11 |
| Cr | 3.7 | ND |
| Cu | 0.22 | ND |
| Fe | 332 | ND |
| P | 8.1 | ND |
| S | 4.6 | 7.3 |
| Ti | 2.9 | ND |
| Zn | 2.4 | ND |
| Be | 0.015 | 0.002 |
| Mo | ND | 0.06 |
| Sn | ND | 0.09 |
| Cl | NA | 2.5 |
| NO ₃ -N | NA | 0.06 |
| SO ₄ | NA | 11.3 |
| F | NA | 0.6 |

^a concentrations are in mg/L

ND - Not Detected

NA - Not Analyzed

The leachate from sample S3 had overall higher concentrations in almost all the detected elements except for Mo and Sn. The high concentrations are attributed to the acid used for the leaching experiment and also to the final low pH of the leachate. The initial acid solution had a pH below 1.7. Therefore, it is more capable of dissolving the slag matrix than distilled water (pH = 6.0). The final pH of the leachate of sample S3 was 1.7. At this low pH, metals remain in solution rather than precipitate.

Relatively high concentrations for Ca, Mg, Si, Al, and Fe were recorded in the leachate of sample S3. The concentrations of Mg, Mn, Si, were over 100 mg/L whereas that of Fe was 332 mg/L. Ca had an even higher concentration (739 mg/L). The composition of the leachate generally reflects the composition of the slag material. However, there are elements like Si that are not subject to release to solution because they are more greatly bonded to the slag matrix. Therefore it is expected that Ca, being a relatively mobile element, will have a higher potential for release than Si.

The source of Ca is from the dissolution of β' Ca_2SiO_4 (larnite). Fe originates from FeO (wustite). The relatively high glass content of the steel slag, as determined by the microscope studies, also contributes to the composition of the leachate.

The leachate of sample S4 yielded Ca, Si, and S as the major constituents. The source for these elements is from the dissolution of $\text{Ca}_3\text{Mg}(\text{SiO}_4)_2$ (merwinite) and β' Ca_2SiO_4 (larnite). SEM/EDS analysis revealed the presence of S that is possibly associated with that phase or with the glass. "Merwinite" also contains Mg that is found in the leachate in smaller concentrations.

Mo and Sn were identified in the solution. It is difficult to trace the source of these two metals since the SEM failed to detect them. It is possible that these two metals were added as

part of the steelmaking process, like V and Cr, to improve the properties of steel. They could be located in the glass phase or as substitutes for Fe and Mg in $\text{Ca}_3\text{Mg}(\text{SiO}_4)_2$ (merwinite). The elevated concentration of Mo in well #2 groundwater (Table 1) could be explained by the weathering of the steel slag. Mo is also found in petroleum products that are also present in groundwater near well #2. Sr can substitute Ca in $\text{Ca}_3\text{Mg}(\text{SiO}_4)_2$ (merwinite) and in β' Ca_2SiO_4 (larnite). The Sr in steel slag could originate from the limestone or dolomite used in the blastfurnace as part of the steelmaking process. The source of P and S could be from the coke used as fuel in the blastfurnace. Figure 12 is a diagram that compares the concentrations of the elements identified with the ICP method between the steel slag leachates and the groundwater chemistry of well #2.

The release of a component per unit mass waste can be calculated by using the equation adopted from Ham et al. (1979b).

$$\text{Release}_{\text{elution}} = (\text{conc, mg/L}) (\text{leachate volume, mL}) (1\text{L}/1000\text{ml}) \\ (\text{dry weight of solid in test, g}) (1\text{kg}/1000\text{g})$$

With this equation, the release of every element into solution per unit mass waste was calculated and is provided in Table 8.

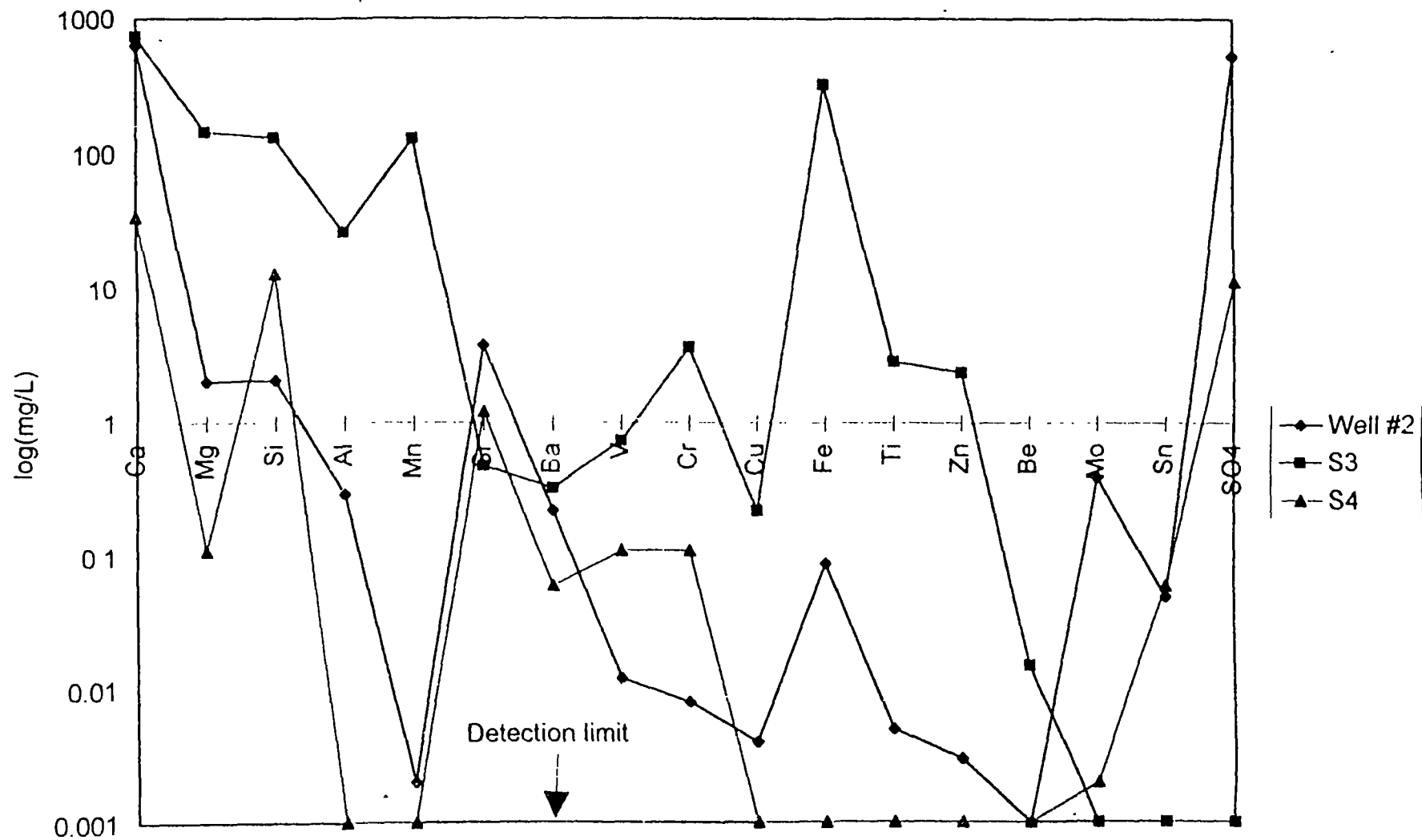


Figure 12. Comparison of chemical constituents of field sample leachates and well #2 groundwater

TABLE VIII

METAL RELEASE PER UNIT MASS WASTE OF
FIELD SAMPLE LEACHATES^a

| Element | S3 | S4 |
|--------------------|-------|-------|
| Ca | -1.51 | -3.25 |
| Mg | -2.22 | -5.76 |
| Si | -2.26 | -3.68 |
| Al | -2.95 | ND |
| Mn | -2.27 | ND |
| Na | -3.93 | -4.71 |
| Sr | -4.71 | -6.02 |
| Ba | -4.88 | -5.76 |
| V | -4.52 | -5.76 |
| Cr | -3.81 | ND |
| Cu | -5.04 | ND |
| Fe | -1.86 | ND |
| P | -3.47 | ND |
| S | -3.72 | -3.94 |
| Ti | -3.92 | ND |
| Zn | -4.00 | ND |
| Be | -6.21 | -7.50 |
| Mo | ND | -6.02 |
| Sn | ND | -5.84 |
| Cl | NA | -3.4 |
| NO ₃ -N | NA | -5.02 |
| SO ₄ | NA | -2.74 |
| F | NA | -4.02 |

^a log values

ND - Not detected

NA - Not Analyzed

4. Geochemical modeling results

Speciation - solubility modeling was performed on the results of the chemical analyses of the leachate obtained from the distilled water leaching experiment and on the well #2 groundwater. The modeling was done with MINTEQA2/PRODEFA2 version 3.0, a geochemical assessment model for environmental systems (Allison et al., 1991). MINTEQA2 is a geochemical equilibrium speciation model capable of computing equilibria among the dissolved; adsorbed, solid, and gas phases in an environmental setting. The model can also provide thermodynamic information of any phase that might be present in the system.

The temperature of calculation was set at 25 degrees C (the temperature of the leaching experiment). In all simulations, no solids were allowed to precipitate from the system. The pH was fixed at the final pH of the leachate (10.7 pH units). The concentrations of the dissolved species were input in mg/L. There were no measurements of the alkalinity of the system, but the partial pressure of CO₂ was fixed arbitrarily at 0.00003 atm. This allowed the saturation indices of carbonates to be estimated, with the partial pressure of CO₂ about 10 % of that in the atmosphere at sea level.

After modeling, the charge imbalance in terms of the percent difference between the sum of anions and cations was relatively high (99.94 %) because anions were not analyzed properly. The ionic strength of the solution was 0.4303. The percentage distribution of the components in solution are summarized in Table 9.

TABLE IX

PERCENTAGE DISTRIBUTION OF COMPONENTS

| | | |
|---------------------------------|-------|--|
| F ⁻ | 100.0 | PERCENT BOUND IN F ⁻ |
| Ca ²⁺ | 5.6 | PERCENT BOUND IN Ca ²⁺ |
| | 94.0 | PERCENT BOUND IN CaCO _{3(AQ)} |
| Mg ²⁺ | 8.0 | PERCENT BOUND IN Mg ²⁺ |
| | 91.0 | PERCENT BOUND IN MgCO _{3(AQ)} |
| H ₄ SiO ₄ | 7.8 | PERCENT BOUND IN H ₄ SiO ₄ |
| | 71.5 | PERCENT BOUND IN H ₃ SiO ₄ ⁻ |
| | 20.7 | PERCENT BOUND IN H ₂ SiO ₄ ²⁻ |
| Na ⁺ | 50.6 | PERCENT BOUND IN Na ⁺ |
| | 48.9 | PERCENT BOUND IN NaCO ₃ ⁻ |
| Sr ²⁺ | 99.9 | PERCENT BOUND IN Sr ²⁺ |
| Ba ²⁺ | 99.9 | PERCENT BOUND IN Ba ²⁺ |
| V ³⁺ | 100.0 | PERCENT BOUND IN V(OH) _{3(AQ)} |
| S | 100.0 | PERCENT BOUND IN S |
| Be ²⁺ | 100.0 | PERCENT BOUND IN Be ²⁺ |
| Cl ⁻ | 100.0 | PERCENT BOUND IN Cl ⁻ |
| NO ₃ ⁻ | 100.0 | PERCENT BOUND IN NO ₃ ⁻ |
| SO ₄ ²⁻ | 99.9 | PERCENT BOUND SO ₄ ²⁻ |
| CO ₃ ²⁻ | 86.5 | PERCENT BOUND IN CO ₃ ²⁻ |
| | 13.1 | PERCENT BOUND IN HCO ₃ ⁻ |
| H ⁺ | 104.1 | PERCENT BOUND IN HCO ₃ ⁻ |
| H ₂ O | 99.1 | PERCENT BOUND IN OH ⁻ |

The saturation index for “calcite” was 2.28, “dolomite” . 2.483, “quartz” -0.395, “monticellite” . -3.825, “larnite” . -10.567, and “merwinite” . -13.522. The saturation index is a logarithmic ratio of the ion activity product (IAP) and the corresponding formation constant after the aqueous phase equilibrated. When the saturation index is positive the mineral phase will be stable and tend to precipitate, otherwise it will be unstable and tend to dissolve. Therefore “calcite” and “dolomite” will be likely to precipitate out of solution, whereas “monticellite”, “larnite”, and “merwinite” will be unstable.

Geochemical modeling with MINTEQA2 was also performed for well #2 groundwater of the May 1991 sampling round (data from Table 1). The solution pH was fixed to 12, the temperature at 25 degrees C, the units of concentration were expressed as mg/L and no solids were allowed to precipitate out of the system. There were no adsorption models specified for the system and the method of computing activity coefficients was the Davies equation :

$$\log \gamma_i = -Az_i^2 \left[I^{1/2} / (1 + I^{1/2}) - 0.24I \right] \quad \text{where } A \text{ is a constant equal to } 0.509 \text{ at } 25^\circ\text{C, } I \text{ is the solution ionic strength, and } z_i \text{ is the charge on each species } i$$

The model produced a low percent difference between the sum of cations and anions (1.9 %). The calculated molarity of $\text{CO}_{2(g)}$ in groundwater was $2.11 \times 10^{-9} \text{ mol/L}$. The activity of CO_3^{2-} is relatively high (0.0015 mol/L) which is in agreement with the high pH values of the solution. 33 % of CO_3^{2-} is bound in CO_3^{2-} , 47 % in $\text{CaCO}_{3(aq)}$, and 20 % in NaCO_3^- (the activity of Na in groundwater is high). The activity of Ca^{2+} is also high (0.0033 mol/L). The saturation indices of CaCO_3 and $\text{CaMg}(\text{CO}_3)_2$ are 3.16 and 2.57, respectively. The positive values of the saturation indices suggest that CaCO_3 and $\text{CaMg}(\text{CO}_3)_2$ will be stable and likely to precipitate. On the other hand, the saturation indices for “larnite”, “merwinite”, and “akermanite” (main mineral phases in

slags) are negative, suggesting that they are not stable under the geochemical conditions of well #2 groundwater. However, the saturation index of “monticellite” which is another common phase in the slag found in situ is 1.28.

B. Blastfurnace slag from Koch Materials

1. X-ray diffraction results

XRD analysis revealed the presence of $\text{Ca}_2\text{MgSi}_2\text{O}_7$ (“akermanite”) as the only phase. Table 10 provides the d-spacings of the sample compared to the ones retrieved from the JCPDS files. XRD methods are relatively insensitive to phase concentrations of less than 5 %. The X-ray powder diffractometer yielded clear and relatively high peaks of “akermanite”. No other peaks were identified. Clear and sharp peaks indicate that the phase is well crystallized, considerably better in the blastfurnace slag than in the field samples of steel slag collected from well #2.

The most common phase in blastfurnace slag is “melilite”, a name applied to any of a series of solid solutions from $\text{Ca}_2\text{MgSi}_2\text{O}_4$ (akermanite) to $\text{Ca}_2\text{Al}_2\text{SiO}_6$ (gehlenite). “Akermanite”, found in the samples, is the Mg-rich melilite. “Akermanite” could also contain Al (up to 4 % of the total weight), Na, Mn, Cr, and Ti substituting for Mg in its structure.

TABLE X

d SPACING AND RELATIVE INTENSITIES OF
BLASTFURNACE SLAG SAMPLES

| JCPDS Files | | | FS1 | |
|---------------------|---------|------------|------------|---------|
| d Å | Rel I % | Phases | d Å | Rel I % |
| 2.87 | 100 | Akermanite | 2.86 | 100 |
| 3.09 | 23 | Akermanite | 3.08 | 21 |
| 1.76 | 20 | Akermanite | 1.76 | 27 |
| 2.48 | 15 | Akermanite | 2.47 | 16 |
| 2.04 | 13 | Akermanite | 2.04 | 23 |
| 5.54 | 9 | Akermanite | 5.52 | 9 |
| 2.39 | 8 | Akermanite | 2.39 | 18 |
| --- | --- | --- | 3.71 | 25 |
| Phases identified : | | | Akermanite | |

--- : Peak Absent

2. Optical and electron microscopy results

The fresh blastfurnace slag samples were analyzed with the SEM/EDS system on selected points from the samples. Table 11 provides SEM/EDS analyses of sample FS1A. Each column (Table 11) represents a point randomly chosen from the thin section. EDS was used to derive the elemental composition with Bence-Albee correction procedures. The results indicate

chemical homogeneity of the sample. They also confirm the XRD identification of one phase (“akermanite”)

The proportionality of each element of point FS1A-A yields 2 for Ca, 0.4 for Al, 0.8 for Mg, 1.8 for Si, and 7 for O. This comes out as $\text{Ca}_2\text{Al}_{0.4}\text{Mg}_{0.8}\text{Si}_{1.8}\text{O}_7$, resembling the chemical formula of melilite which confirms the XRD analysis. SEM/EDS analysis of the same point indicated low concentrations of Na, Mn, Fe, Ti and S.

3. Batch powder-reaction results

Three sets of batch powder-reaction experiments were performed using the blastfurnace slag. In the first experiment, 3.13 g of fresh blastfurnace slag was mixed with 59.16 ml of Milli-Q distilled water resulting to a solid to water ratio of 1 : 18. The pH of the solution was measured over 24 hour periods for about 3 weeks. The solution pH showed a remarkable increase after a short time period of mixing. The solution was kept in 50 ml bottles with airtight lids to prevent mixing of atmospheric gases. The results of this experiment are shown in table 12.

TABLE XI

SEM/EDS ANALYSES OF BLASTFURNACE SLAG (FS1A)

| CALC'D WT % | FS1A-A | FS1A-B | FS1A-C | FS1A-D | FS1A-E | FS1A-F | Average |
|--------------------------------|--------|--------|--------|--------|--------|--------|---------|
| SiO ₂ | 38.13 | 38.80 | 37.08 | 37.63 | 36.27 | 38.74 | 37.77 |
| TiO ₂ | 0.15 | 0.00 | 0.00 | 0.00 | 0.14 | 0.00 | 0.05 |
| Al ₂ O ₃ | 6.71 | 6.37 | 6.87 | 6.96 | 6.89 | 6.03 | 6.64 |
| FeO | 0.13 | 0.13 | 0.23 | 0.17 | 0.10 | 0.14 | 0.04 |
| MnO | 0.27 | 0.11 | 0.87 | 1.19 | 0.78 | 0.13 | 0.56 |
| MgO | 10.57 | 10.36 | 10.25 | 9.83 | 9.75 | 10.21 | 10.16 |
| CaO | 37.91 | 37.94 | 38.17 | 38.39 | 38.75 | 37.71 | 38.14 |
| Na ₂ O | 0.54 | 0.44 | 0.68 | 0.44 | 0.42 | 0.36 | 0.48 |
| K ₂ O | 0.21 | 0.30 | 0.24 | 0.43 | 0.33 | 0.21 | 0.29 |
| Cr ₂ O ₃ | 0.10 | 0.18 | 0.14 | 0.00 | 0.00 | 0.09 | 0.08 |
| NiO | 0.00 | 0.00 | 0.00 | 0.10 | 0.00 | 0.00 | 0.02 |
| SO ₃ | 0.24 | 0.18 | 2.98 | 3.83 | 4.10 | 0.13 | 1.91 |
| P ₂ O ₅ | 0.00 | 0.00 | 0.00 | 0.00 | 0.00 | 0.00 | 0.00 |
| Total | 94.96 | 94.80 | 97.50 | 98.98 | 97.53 | 93.74 | 96.14 |

TABLE XII

pH MEASUREMENTS OF FRESH BLASTFURNACE SLAG

| date | time | pH ^a |
|--------|-------|--------------------|
| 27-Jun | 14:00 | 11.23 ^b |
| 28-Jun | 14:25 | 11.22 |
| 29-Jun | 15:15 | 11.34 |
| 30-Jun | 15:50 | 11.38 |
| 1-Jul | 15:40 | 11.39 |
| 2-Jul | 16:15 | 11.44 |
| 3-Jul | 16:50 | 11.43 |
| 8-Jul | 16:50 | 11.61 |
| 15-Jul | 16:05 | 11.43 |

^a pH units^b pH Measurements after 24 hours of mixing

The slag material is highly alkaline. The solution pH rises to 11.01 after only 20 minutes of mixing. After 24 hours of mixing, the pH of the solution increased to 11.2 units. The dissolved metals in the leachate solutions were analyzed with ICP-AES. Based on their concentrations, they can be separated to major, minor constituents, and trace metals. Major constituents are Ca, Mg, Si, Mn, K, and Na. Minor constituents are Al, Sr, Ba, and V. Trace metals are Fe, Cu, Cr, and Zn. Anions are F⁻, SO₄²⁻, PO₄³⁻, and Cl⁻. NO₃⁻ was not included in the analysis, because HNO₃ was used to acidify the leachate

Analyses for metals and anions were conducted at Argonne National Laboratory, Illinois using inductively-coupled plasma emission spectroscopy (ICPE). The concentrations of the oxides series (leachates exposed to the atmosphere) of major, minor, trace metals and anions are given in the Table 13.

The release of a component per unit mass waste was mentioned in the discussion of the batch powder-reactions of the steel slag samples. The calculated releases into solution per unit mass waste (unitless) of the fresh blastfurnace slag are provided in table 14.

The highest release is observed for Ca in leachate fs1(1) with a value of -1.59 (log units) per unit mass. Fe and Cu have the lowest release in log units per unit mass waste with only -6.50 and -6.80 respectively. Ca is readily available when the slag reacts with solution whereas Fe is not. The results obtained from the anoxic set of experiments (leachate isolated from the atmosphere) are summarized in Table 15. The calculated releases into solution per unit mass waste are provided in table 16.

TABLE XIII

CHEMICAL ANALYSIS OF FRESH BLASTFURNACE SLAG LEACHATE ^a
OXIC SERIES

| Sample | Initial pH | Final pH | Ca | Mg | Si | Fe | Mn | K |
|-----------------------|------------|----------|-------|------|------|------|------|------|
| fs1(1) | 1.15 | 7.9 | 1610 | 314 | 73.1 | 0.02 | 73.6 | 32.2 |
| fs1(2) | 2.04 | 8.5 | 214 | 32.7 | 23.4 | 0 | 4.67 | 21.6 |
| fs1(3) | 3.1 | 9.76 | 68 | 6.59 | 6.67 | 0 | 0.05 | 22.4 |
| fs1(4) | 3.95 | 9.39 | 49.8 | 6.79 | 8.18 | 0.02 | 0.1 | 22.6 |
| fs1(5) | 5.02 | 8.72 | 41.7 | 12 | 8.76 | 0 | 0.17 | 22.9 |
| fs1(6) | 5.98 | 8.9 | 41.3 | 9.12 | 6.63 | 0 | 0.12 | 21.4 |
| fs1-diss | | | 541 | 132 | 377 | 3.53 | 11.7 | 6.44 |
| % weight ^b | | | 26.26 | 6.41 | 18.3 | 0.17 | 0.57 | 0.31 |

| Sample | Na | Al | Sr | Ba | V | Cr | Cu | Zn |
|-----------------------|------|------|-------|-------|------|--------|--------|--------|
| fs1(1) | 42.7 | 0.41 | 1.97 | 1.05 | 0.14 | 0.05 | 0.06 | 0 |
| fs1(2) | 33.8 | 0.16 | 0.28 | 0.33 | 0.06 | 0.01 | 0.03 | 0 |
| fs1(3) | 33 | 0.23 | 0.15 | 0.15 | 0.02 | 0 | 0 | 0 |
| fs1(4) | 32.8 | 0.34 | 0.14 | 0.14 | 0.02 | 0 | 0 | 0 |
| fs1(5) | 34.6 | 0.13 | 0.14 | 0.12 | 0.04 | 0 | 0.01 | 0 |
| fs1(6) | 33.5 | 0.15 | 0.13 | 0.1 | 0.03 | 0 | 0 | 0 |
| fs1-diss | 5.19 | 8.92 | 0.84 | 0.75 | 0.21 | 0.12 | 0.11 | 0.06 |
| % weight ^b | 0.25 | 4.33 | 0.041 | 0.036 | 0.01 | 0.0058 | 0.0053 | 0.0029 |

| Sample | F ⁻ | Cl ⁻ | PO ₄ ³⁻ | SO ₄ ²⁻ |
|--------|----------------|-----------------|-------------------------------|-------------------------------|
| fs1(1) | <1 | 68 | <10 | 89 |
| fs1(2) | 1.8 | 68 | <10 | 52 |
| fs1(3) | 1.5 | 66 | <4 | 44 |
| fs1(4) | 1.6 | 64 | <2.5 | 46 |
| fs1(5) | 1.8 | 66 | <2.5 | 47 |
| fs1(6) | 1.6 | 65 | <2.5 | 47 |

^a concentrations are in mg/L

^b The % weight refers to the elemental form in the bulk initial solid

TABLE XIV

METAL RELEASE PER UNIT MASS WASTE UNDER OXIC CONDITIONS^a

| Sample | Ca | Mg | Si | Al | Mn | K | Na |
|--------|-------|-------|-----------------|-----------------|-------|-------|-------|
| fs1(1) | -1.59 | -2.3 | -2.93 | -5.43 | -2.93 | -3.28 | -3.17 |
| fs1(2) | -2.47 | -3.28 | -3.43 | -5.27 | -4.13 | -3.46 | -3.27 |
| fs1(3) | -2.96 | -3.96 | -3.96 | -5.68 | -6.10 | -3.44 | -3.28 |
| fs1(4) | -3.1 | -3.96 | -3.89 | -5.62 | -5.80 | -3.44 | -3.28 |
| fs1(5) | -3.17 | -3.72 | -3.85 | -2.84 | -5.56 | -3.43 | -3.26 |
| fs1(6) | -3.17 | -3.82 | -3.96 | -4.16 | -5.72 | -3.47 | -3.27 |
| | Fe | Sr | Ba | V | Cr | Cu | |
| fs1(1) | -6.5 | -4.49 | -4.77 | -5.66 | -6.1 | -6.02 | |
| fs1(2) | 0 | -5.35 | -5.28 | -6.02 | -6.8 | -6.32 | |
| fs1(3) | 0 | -5.62 | -5.62 | -6.49 | 0 | 0 | |
| fs1(4) | -6.5 | -5.66 | -5.66 | -6.49 | 0 | 0 | |
| fs1(5) | 0 | -5.66 | -5.72 | -6.19 | 0 | -6.8 | |
| fs1(6) | 0 | -5.68 | -5.8 | -6.32 | 0 | 0 | |
| | F | Cl | PO ₄ | SO ₄ | | | |
| fs1(1) | 0 | -2.96 | 0 | -2.85 | | | |
| fs1(2) | -4.54 | -2.96 | 0 | -3.08 | | | |
| fs1(3) | -4.62 | -2.98 | 0 | -3.15 | | | |
| fs1(4) | -4.59 | -2.99 | 0 | -3.13 | | | |
| fs1(5) | -4.54 | -2.98 | 0 | -3.12 | | | |
| fs1(6) | -4.59 | -2.98 | 0 | -3.12 | | | |

^a log values

TABLE XV

CHEMICAL ANALYSES OF BLASTFURNACE SLAG LEACHATE ^a
ANOXIC SERIES

| Sample | Initial pH | Final pH | Ca | Mg | Si | Al | Mn | K |
|----------|------------|----------|-------|------|------|------|-------|------|
| fsl(1) | 1.4 | 8.37 | 1440 | 280 | 47.6 | 0.13 | 39 | 31.8 |
| fsl(2) | 2 | 10.86 | 272 | 5.19 | 10.1 | 0.25 | 0.04 | 20.3 |
| fsl(3) | 2.94 | 11.13 | 96.3 | 0.77 | 12.8 | 0.34 | <0.01 | 19.4 |
| fsl(4) | 3.88 | 11.12 | 81.2 | 0.58 | 16.7 | 0.32 | <0.01 | 18.6 |
| fsl(5) | 5.05 | 10.97 | 65.5 | 1.39 | 12.6 | 0.27 | <0.01 | 19.2 |
| fsl(6) | 5.82 | 11.12 | 83.1 | 0.71 | 11.8 | 0.42 | <0.01 | 20.8 |
| fs1-diss | | | 541 | 132 | 377 | 89.2 | 11.7 | 6.44 |
| % weight | | | 26.26 | 6.41 | 18.3 | 4.33 | 0.57 | 0.31 |

| Sample | Na | Ti | Sr | Ba | V | Cr | Cu | Fe |
|----------|------|-------|-------|-------|-------|--------|--------|-------|
| fsl(1) | 45.7 | <0.02 | 1.65 | 0.97 | 0.12 | 0.06 | 0.06 | <0.01 |
| fsl(2) | 34.6 | <0.02 | 0.32 | 0.3 | <0.05 | <0.01 | 0.03 | <0.01 |
| fsl(3) | 32.4 | <0.02 | 0.15 | 0.14 | <0.05 | <0.01 | 0.02 | <0.01 |
| fsl(4) | 30.4 | <0.02 | 0.15 | 0.14 | <0.05 | <0.01 | 0.01 | <0.01 |
| fsl(5) | 32.2 | <0.02 | 0.11 | 0.13 | <0.05 | <0.01 | <0.01 | 0.03 |
| fsl(6) | 32.8 | <0.02 | 0.14 | 0.13 | <0.05 | <0.01 | <0.01 | <0.01 |
| fs1-diss | 5.19 | 5.83 | 0.84 | 0.75 | 0.21 | 0.12 | 0.11 | 3.53 |
| % weight | 0.25 | 0.28 | 0.041 | 0.036 | 0.01 | 0.0058 | 0.0053 | 0.17 |

| Sample | F ⁻ | Cl ⁻ | PO ₄ ³⁻ | SO ₄ ²⁻ |
|--------|----------------|-----------------|-------------------------------|-------------------------------|
| fsl(1) | <1 | 70 | <10 | 128 |
| fsl(2) | 2.2 | 61 | <10 | 79 |
| fsl(3) | 2.2 | 62 | 1.3 | 54 |
| fsl(4) | 1.9 | 57 | <2.5 | 53 |
| fsl(5) | 1.7 | 62 | 1 | 57 |
| fsl(6) | 1.7 | 72 | 1.3 | 59 |

^a concentrations are in mg/L

TABLE XVI

METAL RELEASE PER UNIT MASS WASTE UNDER ANOXIC CONDITIONS^a

| Sample | Ca | Mg | Si | Al | Mn | K | Na |
|--------|-------|-------|-----------------|-----------------|-------|-------|-------|
| fsl(1) | -1.64 | -2.35 | -3.12 | -5.68 | -3.20 | -3.29 | -3.14 |
| fsl(2) | -2.36 | -4.08 | -3.79 | -5.40 | -6.19 | -3.49 | -3.26 |
| fsl(3) | -2.81 | -4.91 | -3.69 | -5.26 | -6.80 | -3.51 | -3.29 |
| fsl(4) | -2.89 | -5.03 | -3.57 | -5.29 | -6.80 | -3.53 | -3.31 |
| fsl(5) | -2.98 | -4.65 | -3.70 | -5.36 | -6.80 | -3.51 | -3.29 |
| fsl(6) | -2.88 | -4.94 | -3.72 | -5.17 | -6.80 | -3.48 | -3.28 |
| Sample | Sr | Ba | V | Cr | Cu | Fe | |
| fsl(1) | -4.58 | -4.81 | -5.72 | -6.02 | -6.02 | -6.80 | |
| fsl(2) | -5.29 | -5.32 | -6.10 | -6.80 | -6.32 | -6.80 | |
| fsl(3) | -5.62 | -5.65 | -6.10 | -6.80 | -6.49 | -6.80 | |
| fsl(4) | -5.62 | -5.65 | -6.10 | -6.80 | -6.80 | -6.80 | |
| fsl(5) | -5.75 | -5.68 | -6.10 | -6.80 | -6.80 | -6.32 | |
| fsl(6) | -5.65 | -5.68 | -6.10 | -6.80 | -6.80 | -6.80 | |
| Sample | F | Cl | PO ₄ | SO ₄ | | | |
| fsl(1) | 0 | -2.95 | 0 | -2.69 | | | |
| fsl(2) | -4.45 | -3.01 | 0 | -2.90 | | | |
| fsl(3) | -4.45 | -3.00 | -4.68 | -3.06 | | | |
| fsl(4) | -4.52 | -3.04 | 0 | -3.07 | | | |
| fsl(5) | -4.57 | -3.00 | -4.80 | -3.04 | | | |
| fsl(6) | -4.57 | -2.94 | -4.68 | -3.03 | | | |

^a log values

There are strong similarities when comparing the oxic and the anoxic concentrations. Leachates fs1(1), fs1(2), and fs1(3) have consistently higher concentrations of major and minor elements in the oxic than in the anoxic set. Leachates fs1(4), fs1(5), and fs1(6) have greater concentrations of major and minor elements in the anoxic rather than in the oxic set. This is explained by the higher pH of the solution of the anoxic set. Certain elements such as Si and Al are more soluble under higher pH conditions. This explains the higher concentrations of these elements when the solution pH is higher. Mg seems to be consistently higher in the oxic set regardless of initial or final pH values of the leachates. K and Na have the same concentrations throughout both experiment series; these elements are independent from the pH of the solution or the presence of dissolved O₂ and CO₂. The above information is summarized in Table 17.

Diagrams (Figures 13 and 14) of the solution pH values and the concentrations of the major constituents are given for the oxic and the anoxic series. The pH of the initial solution before mixing and after 24 hours (final pH) are given.

Ca and Mg are more sensitive to the initial pH than the other elements with the concentrations of these two metals decreasing dramatically (Ca : 1610 to 41.3 mg/L, Mg : 314 to 9.12 mg/L) as the initial pH increases. The initial pH has less effect on the concentration of Si in solution. The most dramatic decrease with pH increase has been observed for Mn (73.6 to 0.12 mg/L).

TABLE XVII

COMPARISON BETWEEN OXIC AND ANOXIC SERIES ^a

| | fs1(1) | | fs1(2) | | fs1(3) | |
|----|--------|--------|--------|--------|--------|--------|
| | OXIC | ANOXIC | OXIC | ANOXIC | OXIC | ANOXIC |
| Ca | 1610 | 1440 | 214 | 272 | 68 | 96.3 |
| Mg | 314 | 280 | 32.7 | 5.19 | 6.59 | 0.77 |
| Si | 73.1 | 47.6 | 23.4 | 10.1 | 6.67 | 12.8 |
| Al | 0.41 | 0.13 | 0.16 | 0.25 | 0.23 | 0.34 |
| Mn | 73.6 | 39 | 4.67 | 0.04 | 0.05 | 0 |
| K | 32.2 | 31.8 | 21.6 | 20.3 | 22.4 | 19.4 |
| Na | 42.7 | 45.7 | 33.8 | 34.6 | 33 | 32.4 |
| Ti | 0 | 0 | 0 | 0 | 0 | 0 |
| Sr | 1.97 | 1.65 | 0.28 | 0.32 | 0.15 | 0.15 |
| Ba | 1.05 | 0.97 | 0.33 | 0.3 | 0.15 | 0.14 |
| V | 0.14 | 0.12 | 0.06 | 0 | 0.02 | 0 |
| Cr | 0.05 | 0.06 | 0.01 | 0 | 0 | 0 |
| Cu | 0.06 | 0.06 | 0.03 | 0.03 | 0 | 0.02 |
| Fe | 0.02 | 0 | 0 | 0 | 0 | 0 |

| | fs1(4) | | fs1(5) | | fs1(6) | |
|----|--------|--------|--------|--------|--------|--------|
| | OXIC | ANOXIC | OXIC | ANOXIC | OXIC | ANOXIC |
| Ca | 49.8 | 81.2 | 41.7 | 65.5 | 41.3 | 83.1 |
| Mg | 6.79 | 0.58 | 12 | 1.39 | 9.12 | 0.71 |
| Si | 8.18 | 16.7 | 8.76 | 12.6 | 6.63 | 11.8 |
| Al | 0.34 | 0.32 | 0.13 | 0.27 | 0.15 | 0.42 |
| Mn | 0.1 | 0 | 0.17 | 0 | 0.12 | 0 |
| K | 22.6 | 18.6 | 22.9 | 19.2 | 21.4 | 20.8 |
| Na | 32.8 | 30.4 | 34.6 | 32.2 | 33.5 | 32.8 |
| Ti | 0 | 0 | 0 | 0 | 0 | 0 |
| Sr | 0.14 | 0.15 | 0.14 | 0.11 | 0.13 | 0.14 |
| Ba | 0.14 | 0.14 | 0.12 | 0.13 | 0.1 | 0.13 |
| V | 0.02 | 0 | 0.04 | 0 | 0.03 | 0 |
| Cr | 0 | 0 | 0 | 0 | 0 | 0 |
| Cu | 0 | 0.01 | 0.01 | 0 | 0 | 0 |
| Fe | 0.02 | 0 | 0 | 0.03 | 0 | 0 |

^a concentrations are in mg/L

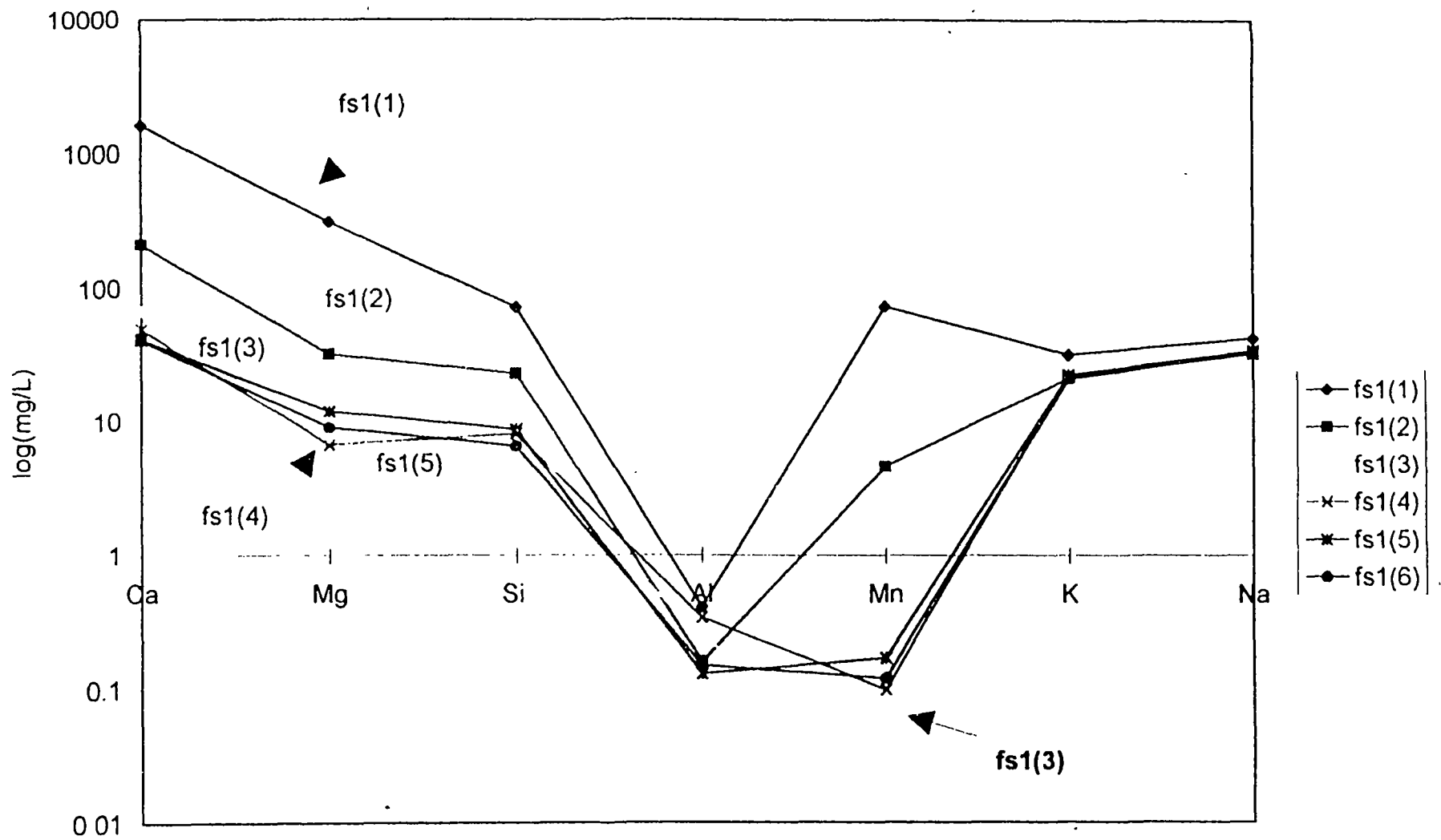


Figure 13 Blastfurnace slag. Batch powder-reaction experiments (Oxic series)

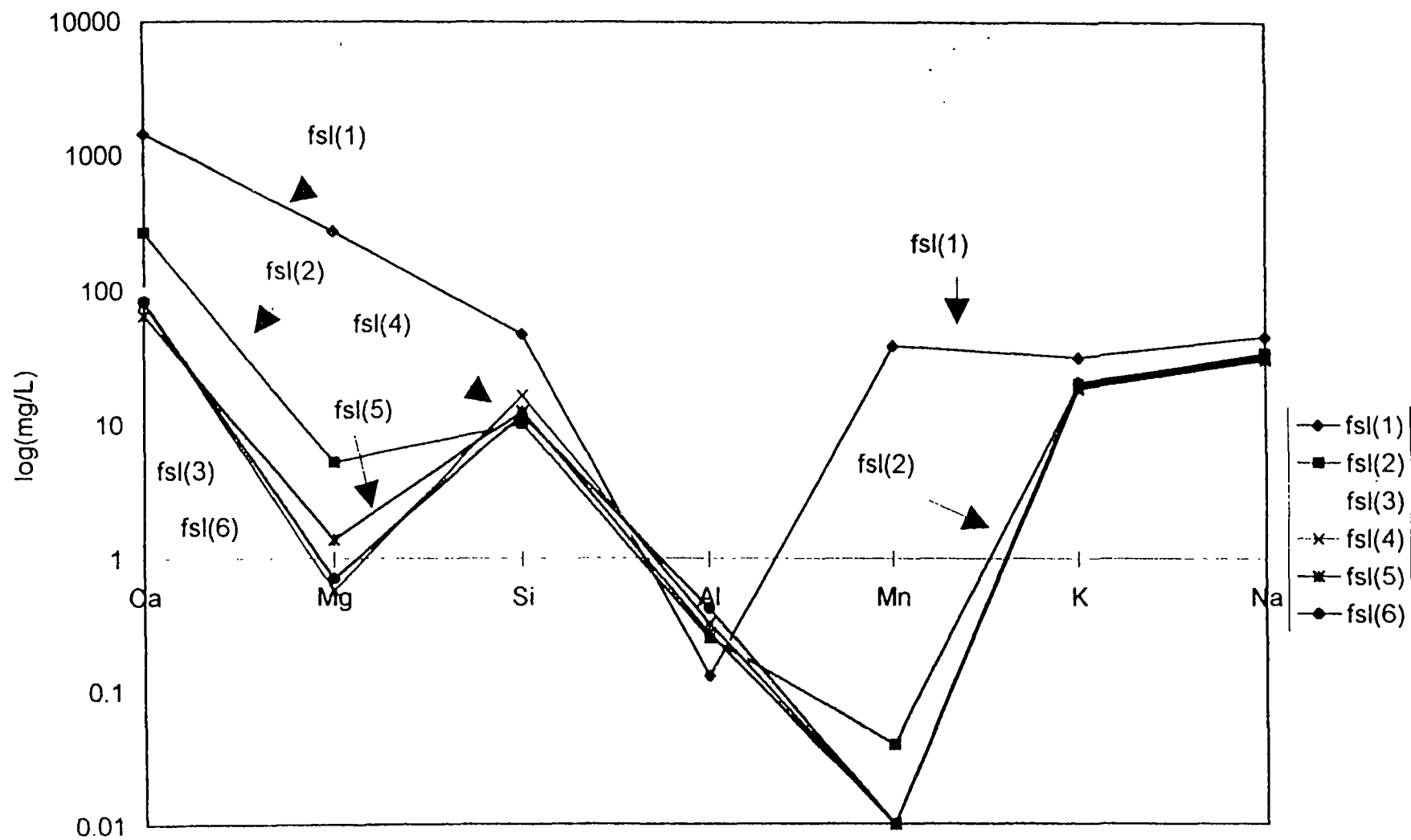


Figure 14. Blastfurnace slag . Batch powder-reaction experiments
(Anoxic series)

4. Geochemical modeling results

Geochemical modeling of the leachates of the fresh blastfurnace slag was performed with MINTEQA2. The leachates of this study are relatively dilute and can be applied to the MINTEQA2 model. This model can predict the equilibrium behavior of metals in a variety of chemical environments. Therefore the movement and transformation of metals can be assessed. MINTEQA2 also provides information on saturation indices for mineral phases.

The total dissolved concentration of all the constituents present in the leachates were included in the model. The temperature was set at 25° C for the oxic series and 15° C for the anoxic. A partial pressure of 0.0003 atm of CO₂ was assumed in the model at the oxic series representing the partial pressure of the gas in the atmosphere. The pH was also fixed to the final pH value of the leachate. No gases were introduced for the anoxic series. No solids were allowed to precipitate out of the system. The ionic strength of the solution is initially unknown and the method used to compute the activity coefficients is the Davies equation.

The concentration of NO₃⁻ is high, as much as 6300 mg/L for FSL-1 and were calculated. The MINTEQA2 model revealed a large difference between the sum of the cations and the sum of anions. This value ranges from 3.47% for FSL-1 to 25.17 % for FSL-6. The sum of anions is always lower despite the fact that NO₃⁻ was used in the calculations.

After running MINTEQA2, the major components present in the leachates of the oxic series is Ca²⁺, Na⁺, Cl⁻, H⁺, CO₃²⁻ and to a lesser extent Mg²⁺, HCO₃⁻, NO₃⁻, and CaSO_{4(aq)}. The saturation indices suggested positive values for “minerals” like “calcite”, “dolomite”, “quartz” and negative values for “akermanite”. Positive values indicate that the solution is oversaturated with respect to these phases and negative values indicate that the solution is undersaturated in respect

to those “minerals”. $\text{Ca}_2\text{MgSi}_2\text{O}_7$ (akermanite) is the sole phase identified with the XRD methods. The MINTEQA2 model suggests that this phase is thermodynamically unstable under the geochemical conditions of the solution.

The saturation indices for “monticellite”, “merwinite”, and “larnite”, which are typical phases in slags, are also negative. An exception is the saturation index of monticellite in leachate FSL-3 where the index is positive. The saturation index has a value of 0.507 which is relatively closer to zero and therefore considered as negative. However the saturation indices of “monticellite”, “merwinite”, and “larnite” have higher values than the corresponding values in the oxalic series. This suggests that higher pH favors the stability of these phases.

The anoxic series presented problems regarding the activity of Al in the final solution. Only samples FSL-1 and FSL-3 were successfully compiled by the program. The computations for FSL-2, FSL-4, FSL-5, and FSL-6 resulted in an estimate of zero for the activity of Al. The major components in the leachates identified by the model were Mg^{2+} , Ca^{2+} , Na^+ , Cl^- and SO_4^{2-} . NO_3^- is also a major component but it originates from the dissociation of HNO_3 . The activity of H^+ is much lower in the anoxic series due to the higher pH values while the activity of CO_3^{2-} is zero due to the absence of dissolved CO_2 .

The saturation index of calcite increases with increasing final pH in the oxalic series of the leaching experiments. When the final pH is 7.9 the saturation index is 0.683. When the final pH reaches the highest value (9.76) in leachate FSL-3 the saturation index of “calcite” also reaches the highest value (2.453). The saturation index of “dolomite” has a similar trend. The saturation index of “quartz” presents a different behavior. It reaches its lower value when the final pH reaches its highest value.

The dissolved concentration of CO_3^{2-} shows an increase with an increase in the final pH. When the final pH is 9.76, in leachate FSL-3, the concentration of CO_3^{2-} is 4.84×10^{-2} mol/kg. This is the highest value among the other leachates of the oxic series. In FSL-3, 64 % of CO_3^{2-} is in the form of HCO_3^- . When the final pH becomes lower the percentage of CO_3^{2-} decreases from 32 % in FSL-3 (pH = 9.76) to 2 % in FSL-2 (pH = 8.5) to zero in FSL-1 (pH = 7.9). The percentage of HCO_3^- on the other hand increases from 64 % in FSL-3 to 93% in FSL-5. The increased concentration of CO_3^{2-} is explained by the higher pH. When the dissolution of slag increases the solution's pH the HCO_3^- releases its H^+ to compensate the decrease of H^+ in the solution as the result of the pH increase. This is why the final pH in the oxic series is always lower than in the anoxic series where dissolved CO_2 is absent.

IV. DISCUSSION

A. Comparison of Steel and Blastfurnace Slag Results

1. X-ray Diffraction Results

The XRD analyses of steel and blastfurnace slags revealed major differences in the composition of phases and in the peak intensities of the x-ray patterns. The steel slag samples included a wide variety of phases (mainly “larnite”, “wustite”, “merwinite”, “monticellite”, and “rankinite”) whereas the blastfurnace slag samples included only one phase (“akermanite”). These phases are all calcium silicates with aluminum and magnesium, and are typical in both types of slag

The other difference was the overall peak intensities. The steel slag samples yielded lower peaks than the blastfurnace slag samples. Optical microscopy revealed a high percentage of glass in the steel slag samples. This suggests the glassy nature of the steel slag material. Therefore, it can be safely assumed that the slag was cooled down rather quickly from high temperature. Despite the low intensity of the peaks they appeared well-resolved. This indicates that the phases were relatively well crystallized but occur in smaller amounts compared to the glass content. The blastfurnace slag samples rendered higher peaks suggesting a relatively high percentage of mineral phases as compared to glass. The blastfurnace slag belongs to the air-cooled type, which may explain the higher crystallinity of the material.

2. Optical and electron microscopy

The steel slag samples appear to be enriched in Fe and Mn compared to the blastfurnace slag samples, and depleted in Ca, Si, and Al, according to the SEM/EDS analysis. SEM photographs of steel slag samples using the BEI mode revealed a relatively heterogeneous composition as demonstrated by the presence of bright and dark areas. This may also explain the theory that in steel slag the reactions between the slag constituents are incomplete (Akiminsuru, 1991b). The blastfurnace slag samples have a more homogenous composition.

The glassy nature of steel slag can also be seen clearly in the optical microscope. Glass is isotropic and opaque to transmitted light. Blastfurnace slag included larger crystals than the steel slag samples.

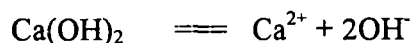
3. Batch powder-reactions

The different bulk chemical compositions of steel and blastfurnace slag resulted in different compositions of their leachates. The different mineral phases are also responsible for the different leachate compositions. Quantitative comparisons between the leachates cannot be made because the amount of solid used in each experiment was different. Also the final pH values of the leachates were different. The steel slag S3 leachate had a pH of 1.7, a relatively low value that resulted in a high concentration of metals in solution. Despite these differences, the leachate of steel slag S3 had higher concentrations of Fe, Mn, and Si and lower concentrations of Na and K than the blastfurnace slag leachates.

B. General nature of slag weathering

The low concentration of Al in the core parts of the steel slag samples may be the result of leaching due to the high pH environment of the groundwater in well #2. Al is insoluble in near neutral pH values and it becomes soluble when the solution pH exceeds ten (Drever, 1988a). This suggestion is consistent with the high concentration of this element in the groundwater system. The Si content in the steel slag is in the range of 30%. The Si content in the groundwater is expected to be high from the elevated pH values but instead is low. It seems possible that some silica or silicate minerals are being precipitated out of solution, probably in the weathered zone of the slag.

The concentration of CaO in steel slag (by mass) usually ranges from 40 to 50% (Lee, 1974b; Reid, 1970). Some of the CaO is in the form of free lime. The concentration of free lime is usually in the range 2-6 % of the total (Turkdogan, 1983). Once in solution CaO (lime) will hydrolyze to Ca(OH)_2 which increases significantly the solution pH as shown in the reactions :



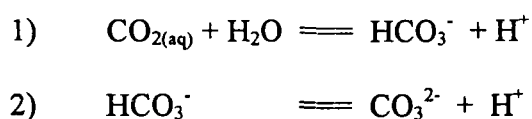
(pH increase)

The relatively high reactivity of CaO in aquatic solutions can account to some extent for the high concentration of Ca^{2+} in well #2 groundwater. Steel slag is invariably heterogeneous due to the presence of undissolved lime. It is possible that the extremely high pH values in wells #2, #3, and #70 could be associated with buried slag that contains a relatively high amount of free lime although no free lime was identified with XRD analysis in the steel slag samples collected from well #2.

Roadcap and Kelly (1994f) observed that the saturation indices of calcite and Mg-calcite decrease dramatically in the high pH wells of the Lake Calumet area. The Ca and Mg likely come from the Ca-rich slag, whereas CO₂ in the groundwater may come from the biodegradation of organic compounds found in well #2 or from inside the slag. The source of carbon in slag is coke used as fuel in the blastfurnace. Carbon can exist in slags as carbide ions (C₂²⁻), especially when conditions in the blastfurnace are strongly reducing and calcium oxides are present in high activities (Richardson, 1974)

No data are available on the concentration of dissolved CO₂ in the field sample leachate. To determine the effects of CO_{2(aq)} on the dissolution of the slag constituents, an arbitrary value for the partial pressure of CO₂ was included in the model. The alkalinity of the groundwater in well #2 was not used in the geochemical modeling of the field sample leachates because it creates an imbalance to the MINTEQA2 model. It is therefore assumed, as mentioned in the Results, that the partial pressure of CO₂ in the field sample leachate (S4) is equal to 3*10⁻⁵ atm.

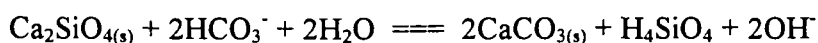
The geochemical modeling of the field sample leachate revealed that CO₃²⁻ has a relatively high activity. This is explained by the hydrolysis of dissolved CO₂ that occurs in two steps :



When the pH of the solution increases, the above reactions will proceed to the right to decrease the pH of the solution. In general, the presence of dissolved CO₂ in groundwater will tend to neutralize the high alkalinity generated from slag weathering.

One of the major cations released from slag weathering is Ca^{2+} . A high pH environment will increase the activity of CO_3^{2-} . The product of the reaction between Ca^{2+} and CO_3^{2-} is CaCO_3 , observed at the slag-water interface. The geochemical conditions present in the groundwater of well #2 (high pH and high Ca content) will favor the precipitation of CaCO_3 .

The phases identified in sample S4 were “merwinite”, “monticellite”, and “larnite”. Ca_2SiO_4 (larnite) can dissolve incongruently in the presence of HCO_3^- in solution according to the reaction :



The Gibbs free energy of the reaction in the standard state (25 degrees C) is $\Delta G^\circ_R = -9.454$ kcal/mol. The equilibrium constant K is related to ΔG°_R by the formula : $\log K = \Delta G^\circ_R / 1.364$. By solving this equation we obtain an equilibrium constant of $K = 8.5 \times 10^6$. The reaction quotient Q for the reaction can be calculated by the formula

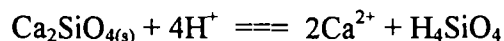
$$Q = [\text{CaCO}_{3(s)}]^2 * [\text{H}_4\text{SiO}_4] * [\text{OH}]^2 / [\text{Ca}_2\text{SiO}_{4(s)}] * [\text{HCO}_3^-]^2 * [\text{H}_2\text{O}]^2$$

The activities of solids ($\text{CaCO}_{3(s)}$ and $\text{Ca}_2\text{SiO}_{4(s)}$) and water are by definition equal to one. The activity values were derived from the geochemical modeling of the leachate with MINTEQA2. By solving this equation we obtain a $Q = 2.04 \times 10^{-8}$ which is substantially lower than the K value, therefore the reaction will proceed to the right and to further dissolve $\text{Ca}_2\text{SiO}_{4(s)}$. With such a high difference between K and Q the reaction is far from equilibrium and only minute amounts of HCO_3^- in solution are sufficient for the incongruent dissolution of $\text{Ca}_2\text{SiO}_{4(s)}$.

The dissolution of Ca_2SiO_4 can be responsible for the increase in the pH of the solution and the precipitation of CaCO_3 (calcite). SEM/EDS analysis revealed that

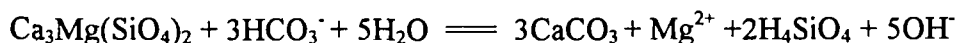
Ca_2SiO_4 contains significant amounts of Mg (7-8 %). Some of the Mg can be incorporated in the “calcite” structure producing “Mg-calcite”. If the ratio $\text{Mg}^{2+}/\text{Ca}^{2+}$ is considerably higher than one, than “dolomite” might form (Drever, 1988b). “Dolomite” was detected in the weathered part of the steel slag samples.

In the absence of HCO_3^- in groundwater “larnite” can dissolve congruently as shown by the reaction :



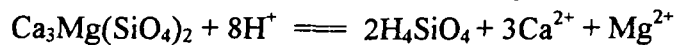
with $\Delta G^\circ_R = -53.16 \text{ kcal/mol}$ and $K = 9.33 \cdot 10^{38}$. The activities of Ca^{2+} , H_4SiO_4 , and H^+ were derived from the modeling of the sample leachate S4 in the absence of CO_2 . The quotient Q of the reaction is $Q = 1.69 \cdot 10^{32}$ which is lower than K , therefore the reaction will proceed to the right increasing the pH, and producing Ca^{2+} and H_4SiO_4 . If conditions are favorable (e.g. decrease in solution pH) the dissolved silica can precipitate as gelatinous amorphous SiO_2 (Faure, 1991) As amorphous silica ages, it recrystallizes to form SiO_2 (quartz), as detected in the weathered part of the field samples

The incongruent dissolution of $\text{Ca}_3\text{Mg}(\text{SiO}_4)_2$ (merwinite) can lead to the formation of CaCO_3 (calcite) as shown by the reaction :



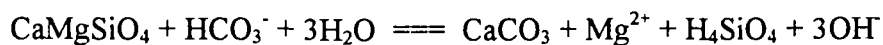
with $\Delta G^\circ_R = -198.17 \text{ kcal/mol}$ and $K = 10^{145}$, a extremely high value. Using the activity values calculated from MINTEQA modeling we obtain a reaction quotient $Q = 4.66 \cdot 10^{-28}$, which is much smaller than K , therefore the reaction will proceed to the right dissolving “merwinite” and increasing the pH even with minute amounts of HCO_3^- in solution

In the absence of HCO_3^- , $\text{Ca}_3\text{Mg}(\text{SiO}_4)_2$ will dissolve congruently as shown in the reaction :



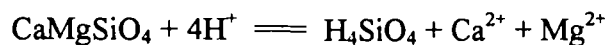
with $\Delta G^\circ_R = -274.92 \text{ kcal/mol}$ and $K = 10^{202}$. The reaction quotient is $Q = 1.38 \times 10^{62}$ which is smaller than K , therefore the reaction will proceed to the right consuming H^+ and increasing the solution pH. As mentioned in the Introduction, the only reactive phase in slag materials that will readily hydrate is Ca_2SiO_4 . Therefore, it is not expected that $\text{Ca}_3\text{Mg}(\text{SiO}_4)_2$ will be subject to weathering to the extent of “larnite”.

In the presence of HCO_3^- , “monticellite” (CaMgSiO_4) dissolves incongruently as shown in the reaction :



with $\Delta G^\circ_R = 18.58 \text{ kcal/mol}$ and $K = 2.39 \times 10^{-14}$. The reaction quotient Q for the leachate of sample S4 is 2.28×10^{-20} . Q is lower than K therefore the reaction has not reached equilibrium and it will proceed to the right dissolving “monticellite” and producing “calcite” and Mg ions. The Mg ions can incorporate in the structure of “calcite” to form “Mg-calcite”.

In the absence of dissolved CO_2 in the leaching media, “monticellite” will dissolve congruently according to :



with $\Delta G^\circ_R = -41.46 \text{ kcal/mol}$ and $K = 2.49 \times 10^{30}$. The reaction quotient Q is equal to $Q = 8.21 \times 10^{29}$ which is almost equal to K . The reaction is near equilibrium but it will proceed to the right dissolving “monticellite” and at the same time increasing the pH of the solution.

A white precipitate was observed at the bottom of ditches that discharge groundwater coming into contact with buried slag material (Figure 15). The same white

(calcite) The increase of water temperature as groundwater discharges to surface water and the decrease of the partial pressure of CO_2 as a result of photosynthesis favors the precipitation of CaCO_3 . Therefore CaCO_3 appears to be the major secondary phase of steel slag weathering



Figure 15 CaCO_3 (calcite) precipitates in ditches near well #2

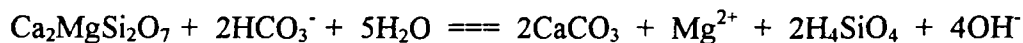
Microscope studies revealed that the weathered zone is consistently less porous than the core part of the slag due to the precipitation of CaCO_3 . Therefore “calcite” could act as a protective coating where it prevents further dissolution of the core part. If conditions change (decrease in groundwater pH) “calcite” becomes unstable, and groundwater could dissolve the calcite coating and penetrate the unweathered slag material. Exposure of “larnite” to groundwater will increase the pH leading to new “calcite” precipitation and attenuation of the weathering.

The chemical compositions of most steel slags exposed to weathering for extended periods are different from those of fresh slags. Akiminsuru (1991c) observed that CaO hydrates rapidly with large volumetric expansion whereas MgO hydrates slowly, expanding over a long period of time. The expansion of these oxides increases the surface area of slag material thus enhancing slag weathering. Therefore the hydration of calcium oxides and the precipitation of calcite appear to be the major weathering mechanisms that act on slag in a landfill.

FeO (wustite) was detected in the core and weathered part of the steel slag samples. “Wustite” does not occur commonly in nature and is found only in steel mill slags and meteorites. SEM/EDS analysis revealed a high content of Mn (9 % by weight) in “wustite”. Dissolved ferrous iron and manganese, derived from the weathering of “wustite”, are not stable at pH values above 7 or 8 in reduced environments. They will precipitate out of solution to either oxyhydroxide or carbonate minerals (Roadcap and Kelly, 1994g). This explains the low concentrations of these elements in the high pH wells of Lake Calumet. The presence of “wustite” in the weathered part of S5 suggests that it

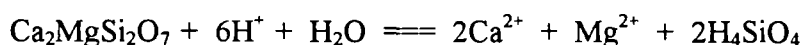
could have been part of the initial slag components that have been transformed by chemical weathering to the components that constitute the outside weathered part

$\text{Ca}_2\text{MgSi}_2\text{O}_7$ (akermanite) detected in the blastfurnace slag samples will dissolve incongruently in the presence of HCO_3^- in groundwater according to :



The Gibbs free energy of the above reaction in the standard state is $\Delta G^\circ_R = 19.055$ kcal/mol and the equilibrium constant $K = 1.07 \cdot 10^{-14}$. The reaction quotient Q can be calculated by using the activities derived from the modeling with MINTEQA2 of blastfurnace slag leachate (FSL-1, oxic series), and $Q = 9.64 \cdot 10^{-26}$ which is less than the equilibrium constant K therefore the reaction will proceed to the right. The dissolved Mg^{2+} can incorporate in the structure of “calcite” and produce “Mg-calcite”. “Dolomite” might form eventually if the ratio $\text{Mg}^{2+}/\text{Ca}^{2+}$ is considerably higher than one (Drever, 1988c).

In the absence of HCO_3^- in groundwater than “akermanite” will dissolve congruently as shown in the reaction



with $\Delta G^\circ_R = -62.83$ kcal/mol (standard state) and $K = 8.71 \cdot 10^{47}$. The reaction quotient for the blastfurnace leachate FSL-1 (anoxic series) is $Q = 2.49 \cdot 10^{38}$ which is lower than the equilibrium constant K , therefore the reaction will proceed to the right consuming $\text{Ca}_2\text{MgSi}_2\text{O}_7$ and increasing the solution pH as demonstrated by the leaching experiments.

The weathering of blastfurnace slag will lead to an increase of the solution pH and the release of Ca^{2+} and Mg^{2+} as major ions that could precipitate as “calcite” and/or “Mg-calcite” in the presence of CO_2 .

C. Potential impact on groundwater chemistry

Groundwater with high pH values has a distinctive chemistry and appears to be associated with the presence of buried steel slag in the Lake Calumet area, based on the well log data. These unusually high pH values are rare in natural water systems and are only found in thermal springs or ultramafic environments (Hem, 1989).

Batch powder-reaction experiments of the steel slag samples collected from the borehole of well #2 were conducted to provide insight to the chemical composition of groundwater in the vicinity of well #2. Some similarities between the steel slag leachates and the well #2 groundwater were determined. The concentrations of Ca, Si, Fe, and S appear relatively high in both the leachates and well #2 groundwater (Figure 12). Relatively high concentrations of Mo were recorded in the leachate of sample S4 as well as in the groundwater. Slags can contain trace amounts of Mo (McGannon, 1964). SEM/EDS analysis did not reveal the presence of Mo but it was detected in the leachate of S4. The relatively high concentration of Mo in the groundwater of well #2 can also be attributed to the high pH values. Stollenwerk (1994) found that the sorption of Mo (IV) by sandy aquifer material decreased as pH, sulfate (SO_4), and phosphate (PO_4) increased.

The concentrations of Al, Sr, Ba, Cu, Ti, Zn, Be, and Sn appear relatively low in the leachates and in the well #2 groundwater. The least-squares method was used to determine the similarities between the leachates and the groundwater. The concentrations of every constituent in the leachate of sample S4 and groundwater was plotted at a XY scatter plot for comparison (Figure 16). The correlation coefficient between the chemical composition of the field sample leachates and well #2 groundwater appeared to be relatively high. The concentrations of Na and Cl were very high as a result of road salt

runoff and were excluded from the analysis. The correlation coefficient between the groundwater and leachate S4 using Ca, Mg, Si, Sr, Ba, V, Be, Mo, Sn, NO₃, SO₄, and F, was $R^2 = 0.7096$.

The comparison between the chemical composition of these steel slag leachates and the existing groundwater chemistry of well #2 is limited in many ways. Two samples cannot account for the entire population of slag material even within the vicinity of well #2.

The sources of the major, minor and trace constituents of groundwater in the vicinity of well #2 can be other than slag. For instance, well #2 is adjacent to the Calumet expressway and receives runoff from de-icing agents used during the winter. Road salt runoff can therefore, account to some extent for the high concentrations of Na and Cl in well #2. The hydraulic character of the man-made fill materials are extremely variable even over short distances and it is therefore risky to delineate groundwater flow paths.

The steel slag near well #2 was buried nearly 70 years ago, surely more than the duration time of the lab experiments. However, a 24 hour experiment may simulate years of leaching in the field. Kinetics can play a crucial role affecting the concentrations of different constituents in the groundwater. Microbial activities and ion exchange mechanisms can also affect the geochemistry of the waters. In the field bacteria may convert hazardous compounds into non-hazardous, or vice versa, or they may alter the leaching characteristics of a waste through their action on the waste matrix (Ham et al., 1979c).

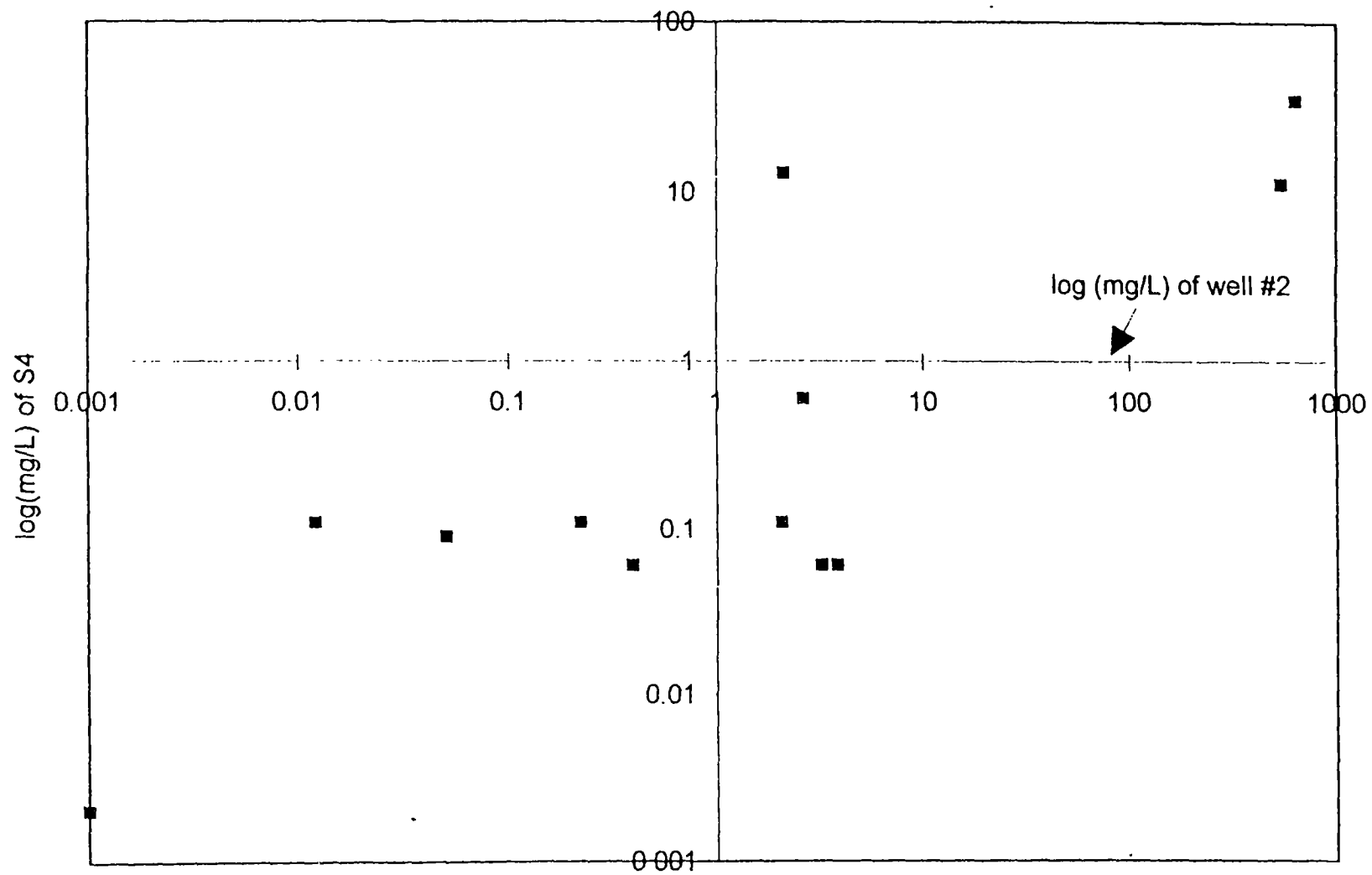


Figure 16 Comparison of chemical compositions of steel slag leachate S4 and well #2 groundwater

The major constituents released from blastfurnace slag are Ca, Mg, Si, K, and Na. The concentrations of Ca, Mg, and Si are controlled by the pH of the leaching media and the pH of the final leachate as well. The concentration of Al and Si were higher in the anoxic series due to the higher pH of the leachate. There were no significant variations in the concentration of K, Na, and Cl with respect to the pH of the solution. This implies that Na and K are in the form of chlorides that are readily available to solution. Trace amounts of Sr, Ba, Mn, and V were detected in the leachates, especially where the pH of the leaching media was low.

CaCO_3 has the ability to adsorb heavy metals depending on the solution pH. The zero point of charge for calcite is reported to lie between the pH values of 8.0 and 9.5, with surfaces having a positive charge below pH 8 and negative charge above 9.5. The pH of the groundwater at well #2 is above 11.0 and therefore calcite will have a negative surface charge. The negative surface charge will attract free cations in groundwater like K^+ , Na^+ , Mg^{2+} , Fe^{2+} or Fe^{3+} , Mn^{2+} , and heavy metals that might also be present like Pb^{2+} , Cd^{2+} , etc. Therefore calcite which appeared as coatings around the slag material and as a precipitate on the bottom of ditches and ponds can inhibit cation mobility in ground and surface water.

The relatively large release of K^+ , and Na^+ can create secondary effects to groundwater. These two cations may release potentially hazardous trace metals through ion exchange mechanisms. Thus, the leachate itself may not be hazardous, but it may liberate hazardous materials in landfill environments.

D. Suggestions for future work

The results of this project suggest several areas for future work. These areas will be important to gain a more complete understanding of the effects of steel mill slags on groundwater chemistry and on the wetlands of the Lake Calumet area. The research can be extended to other areas that have accumulated wastes from the steel mill industries like northwest Indiana. Some of the areas to be considered include .

1) A development of a groundwater potentiometric map so flow paths can be constructed. Consideration should be given to factors such as the annual net infiltration of water, movement of groundwater through the landfill, and the fate of the slag leachate after it leaves the waste and passes through additional wastes or soils.

2) The analyses of background levels of solutes in groundwater and comparison with the leachates from slag weathering. This would require an extensive groundwater monitoring system to delineate groundwater flow paths and to identify potential upgradient sources of contamination that could interfere with the leachate.

3) A mapping of the slag using remote sensing or geophysical methods and information obtained from the well logs to determine the volume of the steel mill slag disposed in the area. The current research has indicated that slag materials along with dredging account for half of the disposed wastes in the 31 square miles of the Lake Calumet area. A more thorough knowledge of the amount of steel mill slag is needed.

4) Investigate the role of the organic contamination in the mobilization of the metals released from slag weathering. Also, examine the role of the secondary minerals from slag weathering in adsorption and ion exchange phenomena.

CITED LITERATURE

- Akiminsuru, J.O.: Potential beneficial uses of steel slag wastes for civil engineering purposes. Resources, Conservation and Recycling, 5:73-80, 1991.
- Ali, A.: Contamination of Alluvial Aquifers by Metal Industries in parts of Central Ganga Basin, India. Wat. Sci. Tech. 26(9-11):2321-2324, 1992.
- Allison, J.D., Brown, D.S., and Novo-Gradac, K.J.: Minteqa2/prodefa2, a geochemical assessment model for environmental systems: version 3.0 user's manual. Environmental research laboratory office of research and development U.S. environmental protection agency, Athens, Georgia, 1991.
- Berner, U.R.: Modeling the Incongruent Dissolution of Hydrated Cement Minerals. Radiochim. Acta 44/45:387-393, 1988.
- Butler, B.C.M.: Al-rich Pyroxene and Melilite in a Blast-furnace Slag and a Comparison with the Allende Meteorite. Mineralogical Magazine 41:493-499, 1977.
- Colten, C.E.: Industrial Wastes in the Calumet Area, 1869-1970. Research Report 001, Illinois Hazardous Waste Research and Information Center, Champaign, IL., 1985.
- Cravens, S.J., and Zahn, A.L.: Ground-Water Quality Investigation and Monitoring Program Design for the Lake Calumet Area of Southeast Chicago. Illinois State Water Survey Contract Report 496, Champaign, 112 pp., 1990.
- Derge, G.: Basic Open Hearth Steelmaking. The American Institute of Mining, Metallurgical, and Petroleum Engineers, Third Edition, New York, 1964.
- Doss, P.K.: Geochemistry of shallow ground water and wetlands in the vicinity of surface-disposed steel-mill slag, Gary, Indiana. Indiana Department of Environmental Management, ARN 93-469, 1996.
- Drever, J.I.: The Geochemistry of Natural Waters, 2nd edition. Prentice Hall, Inc., 1988.
- Faure, G.: Principles and Applications of Inorganic Geochemistry. Macmillan Publishing Company, 1991.
- Ford, M. and Tellam, H.: Source, Type, and Extent of Inorganic Contamination within the Birmingham Urban Aquifer System, UK. J. Hydrol. 156:101-135, 1994.
- Ham, R.K., M. A. Anderson, R. Stegmann, and Stanforth, R.: Comparison of three Waste Leaching Tests, Executive Summary. Special report prepared for the Office of Research and Development, U.S. Environmental Protection Agency, 1979.

- Hem, J.D.: Study and Interpretation of the Chemical Characteristics of Natural Water, 3rd ed U.S. Geological Survey Water-Supply Paper 2254, 1989.
- Lankford, W.T., Jr., Samways, N.L., Craven, R.F., and McGannon, H.E.: The Making, Shaping and Treating of Steel. United States Steel Corporation, Tenth Edition, 1985.
- Lea, F.M.: The Chemistry of Cement and Concrete. London, E. Arnold, 1956.
- Lee, A.R.: Blastfurnace and Steel Slag Production, Properties, and Uses. New York, Wiley, 1974.
- Lewis, R.Sr.: Hawley's Condensed Chemical Dictionary, 12 edition. Van Nostrand Reinhold Company, New York, 1993.
- Mattigod, S.V., Rai, D., Eary, L.E. and Ainsworth, C.C.: Geochemical Factors Controlling the Mobilization of Inorganic Constituents from Fossil Fuel Combustion Residues: I. Review of the Major Elements. J. Environ. Qual. 19:188-201, 1990.
- McGannon, H.E.: The Making, Shaping and Treating of Steel, eighth edition. United States Steel Corporation, 1964.
- Nemerow, N.L.: Industrial Solid Wastes. Ballinger Publishing Company, Cambridge, Massachusetts, 1984.
- Reid, J., Galloway, J.M., MacDonald J., and Bach, B.B.: Rapid Analysis of Slags and Sinters by Atomic Absorption Spectrometry. Metallurgia v81, n48, June 1970, pp 244-247.
- Richardson, F.D.: Physical Chemistry of Melts in Metallurgy, v2. Academic press Inc (London) LTD, 1974.
- Roadcap, G.S., and Kelly, W.R.: Shallow Ground-water Quality and Hydrogeology of the Lake Calumet Area, Chicago, Illinois. Interim report prepared for the Illinois Department of Energy and Natural Resources, Springfield, IL and The United States Environmental Protection Agency, Chicago, IL, 1994.
- Roy, W.R., Seyler, B., Steele, J.D., Mravik, S.C., Moore, D.M., Krapac, I.G., Peden, J.M., and Griffin, R.A.: Geochemical Transformations and Modeling of two Deep-well Injected Hazardous Wastes. Ground Water 29:671-677, 1991.
- Stollenwerk, K.G.: Simulation of Molybdate Sorption with the Diffuse Layer Surface-Complexion Model. U.S. Geological Survey, 1994.
- Turkdogan, E.T.: Physicochemical Properties of Molten Slags and Glasses. The Metals Society, London, 1983.

United States Environmental Protection Agency: Test Methods of Evaluating Solid Waste, EPA method 1310: Extraction Procedure (EP) Toxicity Method and Structural Integrity Test. volume I, section C, Washington D.C., 1986.